DOE/NASA/2593-79/12
NASA TM-79309

EFFECT OF SODIUM, POTASSIUM, MAGNESIUM, CALCIUM, AND CHLORINE ON THE HIGH TEMPERATURE CORROSION OF IN-100, U-700, IN-792, AND MAR M-509

Carl E. Lowell, Steven M. Sidik,
And Daniel L. Deadmore
National Aeronautics and Space Administration
Lewis Research Center

Work performed for
U.S. DEPARTMENT OF ENERGY
Energy Technology
Fossil Fuel Utilization Division

Prepared for
Twenty-fifth Annual International
Gas Turbine Conference sponsored by the
American Society of Mechanical Engineers
New Orleans, Louisiana, March 9-13, 1980

DOE/NASA/2593-79/12
NASA TM-79309

EFFECT OF SODIUM, POTASSIUM, MAGNESIUM, CALCIUM, AND CHLORINE ON THE HIGH TEMPERATURE CORROSION OF OF IN-100, U-700, IN-792, AND MAR M-509

Carl E. Lowell, Steven M. Sidik,
and Daniel L. Deadmore
National Aeronautics and Space Administration
Lewis Research Center
Cleveland, Ohio 44135

Prepared for
U. S. DEPARTMENT OF ENERGY
Energy Technology
Fossil Fuel Utilization Division
Washington, D. C. 20545
Under Interagency Agreement EF-77-A-01-2593

Twenty-fifth Annual International
Gas Turbine Conference sponsored by the
American Society of Mechanical Engineers
New Orleans, Louisiana, March 9-13, 1980

INTRODUCTION

If coal-derived liquids are to become important sources of fuel for power turbines, the effects of trace element impurities on the accelerated corrosion of the turbine must be evaluated. The effects of some of these impurities are known to be adverse. For example, sodium, potassium and vanadium have been identified (Refs. 1-3) by many investigators as being sources of accelerated corrosion when petroleum fuels are burned. On the other hand, some impurities are known to reduce corrosion, e.g., calcium, magnesium (Refs. 4-5). However, there are many impurities whose effects are not known and certainly the effects of the interaction of various impurities are largely unknown. There are two potential approaches to determining the effects of the impurities. The first one is to test many real fuels; by testing a broad spectrum of such fuels the effects of the various impurities from the analyses of the fuels combusted can be inferred. The advantages to this approach are that you use real fuels and the data that one obtains are under conditions closely approaching those found in a real gas turbine. The disadvantages of such tests are that the data obtained are relevant only to the fuels actually tested. Also, currently there are very few liquid coal-derived fuels that are available in quantities sufficient for such tests. The second approach would be to start with the clean fuel and dope it with the impurities of interest in a parametric fashion. The advantage of this approach is that such impurity combinations can be carefully controlled and varied in a systematic fashion allowing the prediction of attack due to any composition. The disadvantages to such tests are that they do not burn real fuel under real turbine operating conditions and that the large number of impurities of interest require many, many tests to be made.

The work described in this report is confined exclusively to the doping approach. The object of this effort is to evaluate the effects of time, temperature, and impurity content on corrosion. The approach used was to burn clean fuels in a burner rig and add aqueous solutions of the impurity combinations required to the combustion gases. The impurities chosen for these tests were sodium, potassium, calcium, magnesium and chlorine. The parametric additions of the impurities were statistically designed to minimize the number of tests. While weight change measurements were made, these data cannot be used to satisfactorily evaluate the extent of hot corrosion attack. The types of deposits were evaluated by X-ray diffraction, while the extent of attack was determined by measuring metal consumption.

MATERIALS

The compositions of the alloys used in this program are listed in Table I. The cobalt base alloy Mar M-509 is a typical vane material which is generally considered to have good hot corrosion resistance due to its high chromium content. The three nickel base alloys turbine blade cover a range of hot corrosion resistance: IN-792 has moderately good hot corrosion resistance, while U-700 has somewhat poorer hot corrosion resistance, and IN 100 has the least resistance to such attack. All of the alloys were cast by a commercial vendor into the shape shown in Figure 1(a). All samples were grit blasted and cleaned with alcohol. Prior to test each sample was measured along a diameter in the center of the expected hot zone (Fig. 1(a)) with a bench micrometer to precision of ± 2 micrometers and weighed to ± 0.2 mg.

PROCEDURE

A burner rig typical of the four used for these tests is shown in Figure 1(b) and has been described in Reference 6. Briefly, each rig is a nominal Mach 0.3 type fired with A-1 jet fuel whose sulfur content was determined to be 0.04 ± 0.01 wt-% over the duration of the tests. The fuel-to-air ratio was varied from about 0.035 to 0.055. The dopants were injected into the combustion chamber as an aqueous solution. Eight samples were rotated rapidly in front of the exhaust nozzle and reached the desired temperature in a few minutes. After each one-hour exposure the burner pivoted away and a forced-air cooling nozzle was directed on the specimens for three minutes. Then this cycle was repeated. After 40 cycles one sample of each alloy was removed and a new sample put in its place. After 100 cycles the samples were removed, weighed, washed, and reweighed. This gave, for each alloy, a sample at 40 hours, 60 hours or 100 hours. Washing consisted of immersion of each sample blade in 300 cc's of water at 80° C followed by a soft brushing in running water, an alcohol rinse, and air drying. The samples were then sectioned along the plane shown in Figure 1(a), which is the center of the hot zone, and where all temperature measurements were made during the run. The cut sections were mounted metallographically, polished and etched. Thickness measurements were made to determine the final thickness at maximum penetration and to calculate maximum metal loss(Y). While both the initial and final thicknesses were measured to precision of 2.5 μm, experience has shown (Ref. 7) that resultant change in thickness is only accurate to about ± 20 μm due to the irregularity of attack and other factors outlined in Reference 7.

The surface of each of the 100-hour samples were scraped for X-ray diffraction analysis. A few milligrams from each sample were obtained and analyzed using a Guinier-deWolff camera. This type of focusing camera was necessary because the complexity of the patterns of the deposits resulted in overlapping diffraction lines.

STATISTICAL DESIGN AND ANALYSIS

Experimental Variables and Plans

The experimental design used in this program is a modification of a class of experimental designs (Refs. 8 and 9). These are all generalizations of plans as illustrated in Figure 2. Figure 2 shows an experiment consisting of two parts, a square (or cube) with a star radiating from the center point. In the cube part, presence of a letter denotes that variable to be at its high level, while absence of a letter indicates the variable is at its low level. The symbol (1) denotes all the variables are at their low level. The extremes of the star are denoted by capital letters with plus or minus.

In the current experiment we consider the seven variables listed in Table II. The original plan consisted of 92 treatment combinations to be run in five groups (blocks). Each block of samples is designed to isolate the effects of certain variables and their interactions. A number of changes were made during the progress of the experiment and the complete list of the observed data is given in Table III. The first four columns of Table III give the observed metal recession for IN 100, U-700, IN-792 and Mar M 509, respectively. The next five columns give the parts per million by weight of combustion gases of Na, K, Mg, Ca and Cl. Column ten gives the test temperatures, and column 11 gives the time of exposure. The last two columns identify the rig on which the test was run and the letter code for the treatment combination as defined above. A number of changes in the test plan were made in the progress of the runs. The first of these resulted from a data review toward the end of block two. Because of the good correlations obtained at that point, blocks three and four were condensed. Block five, consisting of the star points was run in its entirety.

A second condensation came about towards the end of the completion of block two and before the start of block five. At this point a reevaluation of the aims of the program made it clear that the dopants should be considered in terms of elements rather than compounds. This is primarily because it would be difficult, if not impossible, to analytically identify the compound(s) in which the various impurities were present because of the low levels of concentrations found in these fuels.

We therefore redefined the independent impurity variables of interest as parts per million of the elements Na, K, Mg, Ca and Cl. This change had the effect of reducing considerably the orthogonality of the original design. The effect was primarily that Cl was rather highly correlated with Mg and Ca, less highly correlated with Na and K, and had no effect on a correlation of Cl with temperature and with time. However, it did mean that the Cl concentrations tended to be on average considerably higher than the other variables. This approach had little effect on fit of the data.

In order to alleviate this correlation problem and to verify that only the presence of the individual elements matter, several additional runs were made which expanded the scope of the experiment somewhat. These runs are identified by the code EXPAND in column 13 of Table III. In addition, one [illegible] were made with no dopants, that is, oxid[illegible]. These are labeled OXIDAT in column 13 of [illegible]

To illustrate the scope of the program, [illegible]es of parametric plots of the levels of the independent variables have been provided. Not all pairs are plotted, as several such plots are very similar, in particular Figure 4(a) is a plot ppm Na versus ppm Mg. Na vs Cl, K vs Mg, and K vs Ca are very similar and hence not separately plotted. Likewise, Figure 4(b) shows Na vs temperature with K vs temperature being almost identical. Figure 4(c) plots Mg vs temperature with Ca vs temperature being almost identical.

Inclusion of Other Variables

Besides the primary design variables it was necessary to include the possibility that fuel-to-air ratios had an effect on Y (Ref. 10), and that there could be systematic biases from one burner rig to another. The comparison of rig effects can be included by the use of dummy variables. That is, a pair of independent variables R_1 and R_2 are defined such that (R_1, R_2) equals (-1, -1) for rig one, equals (-1, +1) for rig two, equals (+1, -1) for rig three and equals (+1, +1) for rig four. Then the three variables R_1, R_2 and R_1R_2 will reflect the following differences.

R_1 measures (rig 3 + rig 4)-(rig 1 + rig 2)
R_2 measures (rig 2 + rig 4)-(rig 1 + rig 3)
R_1R_2 measures (rig 1 + rig 4)-(rig 2 + rig 3)

Fuel to air ratio was considered as a variable only for the center point runs since it was not recorded in detail for all of the runs.

Uses of the Center Points

The center point of a central composite design is typically repeated a number of times (in this case there were 14 repetitions) during the execution of the overall experiment. The primary reason for this is that since the center point has all the controllable variables held at nominally identical levels, these replicates provide information on: 1) an independent measure of the inherent variability or reproducibility of the results, 2) this error estimate may then be compared to the error estimate obtained from fitting more complicated equations to all of the data to determine if the more general equation is adequate, 3) if the center points are interspersed in time then they can often be used to check for drift or trends that might be occurring due to changing conditions over the course of the runs. The model used for this analysis is $\log r = \beta_0 + \beta_1 X \log \text{time} + \beta_2 f/a + \beta_3 R_1 + \beta_4 R_2 + \beta_5 R_1 R_2 + \varepsilon$.

Full Data Analysis

The fundamental form of the model chosen is a power law in time, that is, $r = a_1 t^{a_2}$ where the rate constant a_1 is a function of the remaining variables, that is, Na, K, Mg, Ca, Cl, time, temperature, and the rigs. More specifically, we use $r = C_1(Na) \cdot C_2(K) \cdot C_3(Mg) \cdot C_4(Ca) \cdot C_5(Cl)\ t^{\beta_1} \exp_{10} (\beta_2 + \beta_3 T + \beta_4 T^2 + \beta_5 R_1 + \beta_6 R_2 + \beta_7 R_1 R_2) + \varepsilon$ where r = metal recession, Na, K, Mg, Ca, Cl = respective dopant levels in ppm, t = time in hours, T = temperature −950° divided 50°, R_1 and R_2 = dummy variables indicating test rig, ε = the unobservable random error and each of the C_i are of the form:

$$C_i = (\theta_{i1} + (1 - \theta_{i1}) \exp(-x\theta_{i2})$$

This functional form has the following properties: a) it is essentially a power law in time so that at time zero there is no attack, b) the impurity functions have the value of unity at 0 concentration and are asymptotic to θ_{i1} as concentrations go to infinity, c) the second order polynomial in the temperature of the exponential term will allow for maximal rate of attack for some temperature if β_4 is less than zero, and d) indicates a belief that the experimental error is proportional in nature rather than additive. It should be pointed out that this type of curve fit requires the use of non-linear regression.

The behavior of this family of impurity functions is indicated in Figure 4. The value of θ_1 is an asymptote such that θ_1 is greater than 1, and the function is monotonically increasing. The parameter θ_2 must be greater than zero and indicates the rapidity of approach to the asymptote. Large values indicate rapid approach and small values indicate slow approach. If θ_1 is less than 1 the function is monotonically decreasing to θ_1. Small values of θ_2 indicate a slow approach and large values a rapid approach.

RESULTS AND DISCUSSION

X-Ray Diffraction of Deposits

As a result of the many different test conditions on four alloys, there is plethora of X-ray diffraction data. These data are presented and discussed in detail in the Appendix. In general, the dopants tended to form the same types of deposits regardless of the concentration or the combinations with other elements. Mg in the combustion products tended to deposit as MgO. Ca, on the other hand reacted with sulfur in the fuel to form primarily Ca sulfate. As expected from other work (Ref. 11) Na and K also deposited as sulfates. In the case of Na, Na_2SO_4 was the primary phase, however, it was found in three separate crystallographic modifications. K, when present in appreciable quantities, was found as K_2SO_4 and it also combined with the Na_2SO_4 to form a mixed sulfate $K_xNa_{2-x}SO_4$. Throughout the analyses a set of unknown lines consistently occurred for which no match could be made with the powder diffraction file. By correlating the presence of these lines with the concentrations of the dopants, we were able to determine that this was probably a phase primarily composed of Na with some K and Ca as a sulfate. This phase was then synthesized as shown in the Appendix and determined to be approximately $Na_6K_2Ca(SO_4)_6$. The above phases accounted for the vast majority of those found in the deposits. Twice a $Na_2Ca_2(SO_4)_3$, glauberite, was found and a few weak lines which were never identified were seen in a few of the patterns.

The presence of these phases presented few surprises, as such sulfate forming reactions have generally been found in these types of tests and have usually led to accelerated corrosion. This is especially true in the cases of Na and K sulfates and their mixtures. The complications introduced by the Na, K sulfates and the Na, K, Ca sulfates is that these compounds form liquid deposits over temperature ranges which are largely unknown. As will be seen from the discussion of the metal recession data, high metal recessions are associated, as would be expected, with large concentrations of Na and K sulfates.

Metal Recession Data - Center Point Analysis

Plots of the raw data for the center points are given on log-log scale in Figure 5. The plots are done separately for each rig. Table IV presents the results of the regression analysis for each alloy.

The analysis of the IN-100 center point data indicates that the exponent of time is (within sampling error), = 1. This would indicate the corrosion is proceeding via a surface reaction. Such reactions would indicate that no protective layer is being formed during the corrosion process and would probably result in highly accelerated corrosion, and indeed IN-100 is known to be a very corrosion-prone material (Ref. 11).

The coefficient of the fuel-to-air ratio is negative by a significant amount indicating that as fuel-to-air increases at this temperature the corrosion rate decreases. These results are not in agreement with the fuel-to-air ratio effects observed on Mar M-509 as shown in Reference 10, and indicate that, quite probably, fuel-to-air as a variable, like so many other variables as found in Reference 11, affect different alloys differently.

The coefficients of the rig effects imply that rigs one and two are similar as are rigs three and four, but the two sets differ significantly. This difference is apperent from the raw data plots of Figure 5. It is interesting to note that rigs 1 and 2 are combined on one table in the laboratory and and rigs 3 and 4 are on another table. While nominally all four rigs are built to the same specifications and presumably identical, it is quite obvious from the data that rig to rig variations do exist at a level significant enough to be detected in this type of experiment.

The variance and the standard deviation estimates are 0.0142 and 0.119, respectively. The approximate

95% confidence limits derived from chi-square distributions are 0.0099. This is less than or equal to the variance which is less than or equal to 0.0219. These limits are given in Table V. When fitting the log of metal recession, the estimate of standard deviation can be used to provide approximate proportional error limits on r. For example, the distribution of log r values for a fixed time, fuel-to-air ratio, and rig has a standard deviation, σ, so that $\log(r) \pm 2\sigma$ is estimated by the $\log(\hat{r}) \pm 2\hat{\sigma}$. Upon taking the antilog we find that $\hat{r} \times 10^{\pm 2\hat{\sigma}}$, so that $10^{\pm 2\hat{\sigma}}$ represents proportional error limits. For the IN-100 we obtained 0.58 and +1.73 indicating that two σ limits are from about 42% low to 73% high.

The U-700 center point data indicate that the coefficient of the log time is significantly larger than 1. This indicates a reaction faster than surface controlled, possibly due to alloy depletion effects. The fuel-to-air coefficient is significantly negative and hence indicates decreasing attack with increasing fuel-to-air as was found with the IN-100. There are two significant rig effects with the larger being rigs 1 and 2 vs rigs 3 and 4, again as was found with the IN-100. Proportional 2σ limits there are estimated to be 50% low to 102% high.

The coefficient on time for the center point data of IN-792 is 0.87, only slightly smaller than 1. This could possibly indicate a corrosion process that is partially surface controlled and partly diffusion controlled. The fuel-to-air coefficient is not significantly different from zero and hence, appears to be not involved in the corrosion of this alloy. There is one significant rig effect, being the difference between rigs 1 and 2 and rigs 3 and 4 as found on the preceding two alloys. Proportional 2σ limits are estimated as 42% low and 73% high.

The Mar M-509 center point results indicated a coefficient in time of about 0.6 which is not significantly different from 0.5. This may indicate a primarily diffusion controlled reaction. The microstructure of the attack zone found on the Mar M-509 alloys both in this study (Fig. 6) and in previous work (Ref. 11), indicate that the attack is largely down grain boundaries, presumably requiring the transport over a rather long distance and may be the cause of the low exponent in time.

There is a significant fuel-to-air effect but no significant rig effects were observed. However, as was the case in the other three alloys, the fuel-to-air coefficient was negative in direct contrast to the results found in Reference 10. This may be related to the differences between the two types of experiments in which the referenced work was obtained on stationary samples and the current data are obtained on samples rotated in the manner described above. However, in the absence of further work the anomaly cannot be fully explained. The proportional two σ limits are estimated as 49% low to 95% high.

Analysis of the Full Data Set

The model of the equation was fitted to all the available data for each alloy by a least squares method. The self-consistency of the data was examined by computing the residuals for each available observation. This consists of computing the predicted values of log $\hat{r}$ for each data point and subtracting that from the observed log r. These residuals were examined in sets of 12. Because of the experimental procedure consisting of three pins of each alloy at 40, 60 and 100 hours it is quite possible that there is some correlation structure underlying these 12 observations due to some common uncontrolled unknown variables. Scaled squared distances from the origin of these vectors of dimension 12 were computed, ordered from the smallest to the largest, and plotted on a chi-squared probability scale (see Section 6.6 of Gnanadesikan (Ref. 12) for details). If the residuals ($\log\hat{r} - \log r$) are normally distributed with no significant inability observed of the calculated model to fit the data, the plot should be a straight line. Figure 7 shows the resulting plot which looks somewhat like a straight line except for possibly points e1, F9 and e9. These points were deleted (indicated by A in Table III) and the models refit. The estimated coefficients were not much different. The residuals for this fit were calculated and plotted with the result presented in Figure 8. This plot seems to indicate two different straight lines with points 15, 30, 29 as possible bad points. The two straight lines may be interpreted as indicating two error processes. Upon examining the data points on the steeper of the two lines it appears that almost all of them involve a situation where r of 60 hours is less than r of 40 hours for one or more of the alloys. No other pattern was seen to emerge. After a detailed, two step analysis of the remaining data examination, all the data points labeled B in Table IV were also dropped as being suspect and the models again refitted. These are the results given in Table V. Upon comparison it was be noted that the largest difference is in the estimated σ value. For the models fit to the edited data set, Table V, we obtained σ values much more in accord with the center point fit. This fact along with the fitted equations being quite similar for all three fits, leads us to conclude the results of the use of the edited data yielded the best results.

Errors

Before discussing the relative effects of the variables on each alloy, the estimates of the residual experimental error and the impact of this error on the results to follow will be discussed. The model is of the form $r = a_1 t^{a_2} 10^{\epsilon}$ where ε is a random error. The estimates of Table V which are labeled $\hat{\sigma}^2$ are estimates of the variance of ε. Plus and minus two standard errors about the model equation is thus given by: $a_1 t^{a_2} \times 10^{\pm 2\sigma}$. Table V represents the factors $10^{-2\sigma}, 10^{+2\sigma}$. It is thus seen that approximately 95% of the observations should fall within a factor of two for IN-792 and Mar M-509. The 95% tolerance limit is slightly larger, about 2.5, for IN-100 and U-700. It must be noted that this is strictly true only if the ε are independent and normally distributed, the model as stated is correct, and we know what the true values of a_1, a_2 are. The probability plots of Figures 7 and 8 indicate approximate normality. We are not sure of the choice of the model. It has several features that are desirable but clearly cannot be assumed to be exactly correct. We must allow for the possibility of a future different model being more chemically precise. Due to the rather large experimental error it will be difficult to distinguish among competing models unless: 1) they are grossly different, or 2) we perform very extensive experimentation. All discussion is in terms of the chosen model. We then come to the point that we have only estimated the coefficients. There are errors and uncertainty in each of these, and hence, uncertainty in the fitted equation. There are no exact methods available for quantifying this uncertainty in the case of nonlinear least squares. The existing approximate techniques are cumbersome and of uncertain validity.

What we are most interested in are those variables which cause changes in the depth of attack that are greater than the changes due to random sampling.

Sodium

Increasing sodium levels increase the rate of attack for all four alloys. The increase is especially dramatic for IN-100 and U-700. From Table V, the asymptotic values are for IN-100, 336.4; for U-700, 105.2; for IN-792, 259.4, and for Mar M-509, 2.667. These values are slightly misleading since they are not approached within the sodium levels observed in the experiment, except for Mar M-509. Figure 9(a) shows a rate factor for sodium over the interval 0-5 ppm. Although not plotted, the factor for sodium is 107.8 at 5 ppm; for IN-100, U-700 and IN-792 it is evident that the change in attack over the 0-5 ppm range is considerably larger than the experimental error, while for Mar M-509 the change is close to the error limits. There are evidently real differences between the rate of each alloy also. As an approximation consider that at 2 ppm the predicted factors and the error limits are

	$\tau 10^{-2\hat{\sigma}}$	τ	$10^{+2\hat{\sigma}}$
IN 100	19.7	48.7	120.3
U-700	5.5	13.9	35.4
IN-792	2.5	5.0	10.0
MM-509	.88	1.7	3.3

These results are consistent with published data (Ref. 11) inasmuch as they indicate that increases in sodium are a cause of increasing attack, and that the alloys corrode in approximately the order one would expect, mainly the most corrosion resistant, Mar M-509 through the least corrosion resistant, IN-100.

Potassium

Increasing values of potassium cause increasing rates of attack. The numerical values defining the rate function are given in Table V, and the functions plotted over 0-5 ppm in Figure 9(b). The change in C_k over that range is clearly larger than the random error effects, but appears to be about the same for each alloy.

Magnesium

Increasing magnesium concentrations decreases attack for all but the Mar M-509 alloy. The Mar M-509 alloy indicates essentially no effect over the range plotted, 0-5 ppm, while for the other alloys the change in attack is about the same. Thus, this study would indicate that magnesium is a favorable element as would be concluded from Reference 13, but not especially so. The behavior of IN-100 and IN-792 are very much alike. These results are plotted in Figure 9(c).

Calcium

Calcium appears to be a favorable additive as increasing calcium concentration leads to decreasing attack for all alloys. The numerical values in Table V indicate rate reductions of from 0.195 to 0.607. These limits are nearly achieved within the levels of calcium examined and the factors are plotted from 0-3 ppm in Figure 9(d). For IN-100 and IN-792 there is a very rapid reduction in rate, while for U-700 and for Mar M-509 reduction is not so rapid. Over the range of 0-5 ppm the change in the funciton is larger than the error limits. These data are certainly consistent with the inhibitor data published in Reference 13, which found that calcium decreased corrosion to some degree.

Chlorine

Chlorine also appears to be a beneficial dopant. The numerical values of Table V indicate asymptotic reduction of rate of attack from 0.1856 to 0.4104 depending upon the alloy. Chlorine concentrations range from 0-16 ppm, the rate factors are plotted from 0-10 ppm for each alloy on Figure 20. This indicates the response to be rather similar for each alloy. The reduction in attack due to the chlorine is greater than the error limits. These results are somewhat surprising as earlier work in burner rigs (Ref. 11) indicated that chlorine was probably a cause of accelerated hot corrosion, although the data were certainly not unambiguous. In this case all of the data seems to strongly indicate that chlorine, when present, can be a cause of reduction of hot corrosion and not of acceleration. This is consistent with the results of Smeggil (Ref. 14).

Rigs

One important and disturbing variable to consider is rig effects. The rigs are nominally identical, thus whatever variability there is from one rig to another is a lower bound on the differences that could result between two different labs. This is because many things change from lab to lab, least among them the rigs. In our model the rig effect is included through the inclusion of the two dummy variables, R_1 and R_2. Table VI presents the deviation of each rig from a nominal or mean rig by indicating the value of 10**$(R_1 + R_2 + R_1 R_2)$. It is thus seen that rig 1 tends to yield attack results about 13-24% higher than nominal, while rig 4 yields results about 11-16% lower than nominal. Rigs 2 and 3 are about average in their effect on corrosion attack.

Temperature

The model chosen for the temperature rate factor has the obvious drawback that there are no temperature - dopant interaction terms. It would be expected that Mg would not have an interaction effect over the range of interest. It forms MgO which probably acts only as either an inert solid or as a slight inhibitor (Ref. 13). However, MgO is a solid at all test temperatures. Cl has been shown to remain largely in the gas (Ref. 15) and whether there should be a Cl - temperature interaction is questionable. One would expect Na-, K-, and Ca-temperature interactions as these form sulfates whose dew points and melting points may be in the test temperature range. Since it is generally assumed that accelerated corrosion occurs primarily at temperatures between the melting point and the dew point of the deposits, the composition of the deposit should strongly influence the shape of the temperature - corrosion curve.

At this stage of the development these types of interactions have not been included in the model. Nevertheless, the temperature profiles predicted by the model are in reasonable agreement with the observed data which would indicate that the potential interaction terms are not necessarily first order effects over the temperature range of interest here. Further refinements in the model may include the temperature-dopant interaction terms provided that their effects are greater that the uncertainty in the data.

CONCLUDING REMARKS

An attempt has been made to study the corrosion attack of turbine airfoil alloys as a function of Na, K, Ca, Mg, Cl, temperature, and time utilizing a statistically designed burner rig program. An attack model was developed from these results which, while obviously incomplete, seems to account for most of the important first order effects. As more data become available, modification and refinement of the model should allow greater predictive ability.

Appendix - X-Ray Diffraction Results for Deposits
by Ralph G. Garlick

The Guinier-deWolff focusing camera method was used for analysis of the powder samples. This method was used chiefly because it offers better separation of peaks than the other available methods in the range of lattice spacings where peak overlap often leads to problems in phase identification. This method also offers the advantage of the ability to run 4 samples under the same diffraction conditions at the same time and having the resulting 4 patterns on 1 film for comparison. This is ideal for comparison of deposits on the 4 alloys for the same deposit conditions.

The results of the diffraction analyses are summarized in Table VII. Under each phase the letters indicate the relative intensity of the pattern for that phase compared to other phases present, S indicating strong, M medium, and W weak. The center points are summarized as if they were 1 run, and, although there was some variability in results, the major phases present were substantially the same for all runs. Sampling to get powder for X-Ray analysis was done primarily for analysis of the deposited material and attempts were made to avoid including the substrate oxides formed on the sample. In many cases this was not possible, as indicated in the table. The absense of substrate in the X-Ray sample, therefore does not indicate that none was present on the sample. As expected, substrate oxide was most often present in the IN-100 samples. Na_2SO_4, presented in the Table as 1 phase, was actually various combinations of 3 separate phases - types I, III, and V Na_2SO_4, with types I and V more commonly present. In most cases only 1 type of Na_2SO_4 was present in a sample. The $K_xNa_{(2-x)}SO_4$ formed in many of the samples is a hexagonal phase with a range of composition of at least from $K_{0.67}Na_{1.33}SO_4$ to $K_{1.5}Na_{0.5}SO_4$ with the unit cell increasing in size as the K/Na ratio increases (Ref. 16).

The column designated $Na_8K_2Ca(SO_4)_6$ is an estimate of the formula for a phase (or phases) present in many of the samples. As previously indicated, a set of unknown lines occurred frequently in certain samples. By correlating the presence and relative strength of this pattern with concentrations of dopants it was determined that the phase was probably a sulfate with Na the principle cation, and small amounts of Ca and K also necessary. To synthesize this material, several samples in this composition range were mixed from the components Na_2SO_4, $CaSO_4$, and K_2SO_4. These mixtures were heated at 900°C for 4 hours, cooled and X-Ray diffraction patterns run for the resulting materials. The results are summarized in the three component phase map, Figure 10. The sample with no potassium (Na/Ca/K = 7/2/0) consisted of Na_2SO_4 + $CaSO_4$. All other samples contained the unknown phase, with 2 samples containing only these unknown lines. These samples were those of Na/Ca/K ratios of 8/2/1 and 7/2/1, indicating a range of composition for the unknown phase. We have designated this phase as $Na_8K_2Ca(SO_4)_6$ which certainly represents the approximate composition. The other samples in the synthesis attempt consisted of this phase plus the sulfate one would expect from the composition (e.g. Na_2SO_4 for Na/Ca/K = 8/1/1).

REFERENCES

1. Stringer, J. F., "Hot Corrosion in Gas Turbines," MCIC-72-08, Battelle Columbus Labs., Columbus Ohio, June 1972.

2. Stringer, J. F., "High Temperature Corrosion of Aerospace Alloys," AGARD-AG-200, Advisory Group for Aerospace Research and Development, Paris, 1975.

3. Lunt, R. E., "Hot Corrosion in Gas Turbines," ASME Paper no. 77-WA/Fu-3, Nov. 1977.

4. Lee, S. Y., Young, W. E., and Vermes, G., "Evaluation of Additives for Prevention of High Temperature Corrosion of Superalloys in Gas Turbines," ASME Paper no. 73-GT-1, Apr. 1973.

5. Zetlmeisl, M. J., May, W. R., and Annand, R. R., "Corrosion Inhibitor for Vanadium-Containing Fuels," U. S. Patent 3,926,577, Dec. 1975.

6. Lowell, C. E. and Deadmore, D. L., "Effect of a Chromium-Containing Fuel Additive on Hot Corrosion," Corrosion Science, Vol. 18, 1978, pp. 747-763.

7. Lowell, C. E. and Probst, H. B., "Effects of Composition and Testing Conditions on Oxidation Behavior of Four Cast Commercial Nickel-Base Superalloys," NASA TN D-7705, 1974.

8. Davies, O. L., ed., The Design and Analysis of Industrial Experiments, 2nd ed., rev., Hafner Publ. Co., New York, 1956.

9. Box, G. E. P., Hunter, W. G., and Hunter, J. S., Statistics for Experimenters, An Introduction to Design, Data Analysis, and Model Building, John Wiley and Sons, New York, 1978.

10. Deadmore, D. L.; Lowell, C. E. and Kohl, F. J.: "The Effect of Fuel-to-Air Ratio on Burner-Rig Hot Corrosion," Corrosion Science, Vol. 19, 1979, pp. 371-378.

11. Deadmore, D. L. and Lowell, C. E., "Burner Rig Alkali Salt Corrosion of Several High Temperature Alloys," NASA TM X-73659, 1977.

12. Gnanadesikan, R., Methods for Statistical Data Analysis for Multivariate Observations, Wiley, New York, 1977.

13. Deadmore, D. L. and Lowell, C. E., "Inhibition of Hot Salt Corrosion by Metal Additives," DOE/NASA/2593-78/2, NASA TM-78960, 1978.

14. Kohl, F. J., Stearns, C. A., and Fryburg, G. C., "Sodium Sulfate: Vaporization Thermodynamics and Role in Corrosion Flames," Metal-Slag-Gas Reactions and Processes, Z. A. Foroulis and W. W. Smeltzer, eds., The Electrochemical Society, Inc., Princeton, N.J., 1975, pp. 649-664.

15. Smeggil, J. G. and Bornstein, N. S., "Study of the Effects of Gaseous Environments on Sulfidation Attack of Superalloys," R77-912614-5, United Technologies Research Center, East Hartford, Conn., 1977 (NASA-CR-135368).

TABLE I. - COMPOSITION OF ALLOYS

(All Values are Weight Percent)

ELEMENT	IN-100	U-700	IN-792	MarM-509
Cr	10	14.2	12.7	23
Ni	Bal.	Bal.	Bal.	10
Co	15	15.5	9.0	Bal.
Al	5.5	4.2	3.2	-
Ti	4.7	3.3	4.2	0.2
Mo	3.0	4.4	2.0	-
W	-	-	3.9	7
Ta	-	-	3.9	3.5
Nb	-	-	0.9	-
V	1.0	-	-	-
Mn	-	< .01	-	-
Fe	-	0.1	-	-
Si	-	< 0.1	-	-
Zr	0.6	< .01	0.10	0.5
B	0.014	0.02	0.02	-
C	0.18	0.06	0.2	0.6

TABLE II. - THE SEVEN INITIAL VARIABLES AND THEIR LEVELS

	Star (-)	Cube (-)	Center Point	Cube (+)	Star (+)
A NaCl	.04 PPM	.20	.45	1.0	4.95
B Na_2SO_4	↓	↓	↓	↓	↓
C KCl	↓	↓	↓	↓	↓
D K_2SO_4	↓	↓	↓	↓	↓
E $MgCl_2$	↓	↓	↓	↓	↓
F $CaCl_2$	↓	↓	↓	↓	↓
G TEMP	800°C	900	950	1000	1100

TABLE III. - SUMMARY OF TEST VARIABLES AND RESULTS

t(hr)				PPM					(°C)	(hr)		
IN100	U700	IN792	MM509	NA	K	MG	CA	CL	TEMP	TIME	RIG	ID
317	254	167	195	0.50	0.50	0.45	0.45	3.21	950	40	1	CP0
424	322	188	73	0.50	0.50	0.45	0.45	3.21	950	60	1	CP0
670	708	276	227	0.50	0.50	0.45	0.45	3.21	950	100	1	CP0
260	354	164	109	0.90	0.90	0.45	0.45	3.21	950	40	2	CP0
378	441	202	124	0.90	0.90	0.45	0.45	3.21	950	60	2	CP0
413	787	257	133	0.90	0.90	0.45	0.45	3.21	950	100	2	CP0
195	117	109	47	0.50	0.90	0.45	0.45	3.21	950	40	3	CP0
224	116	197	76	0.50	0.50	0.45	0.45	3.21	950	60	3	CP0
222	132	148	181	0.50	0.50	0.45	0.45	3.21	950	100	3	CP0
2448(1)	4338	1564	1780	0.50	0.90	0.45	0.45	3.21	950	40	4	CPM
1948	6698	1709	988	0.50	0.90	0.45	0.45	3.21	950	60	4	CPM
563	564	709	213	0.50	0.90	0.45	0.45	3.21	950	100	4	CPM
96	84	91	138	1.20	1.20	1.00	1.00	5.90	1000	40	1	BCEFG
126	176	99	105	1.20	1.20	1.00	1.00	5.90	1000	60	1	BCEFG
294	291	131	166	1.20	1.20	1.00	1.00	5.90	1000	100	1	BCEFG
77	56	27	44	0.40	2.00	1.00	1.00	5.90	900	40	2	CDEF
76	87	64	77	0.40	2.00	1.00	1.00	5.90	900	60	2	CDEF
676	658	124	1078	0.40	2.00	1.00	1.00	5.90	900	100	2	CDEF
128	938	1044	988	1.20	1.20	0.20	0.20	3.39	1000	40	3	ACG
1210	1364	838	860	1.20	1.20	0.20	0.20	3.39	1000	60	3	ACG
1658	1998	1724	3048	1.20	1.20	0.20	0.20	3.39	1000	100	3	ACG
87	98	89	126	0.40	2.00	1.00	0.20	4.49	1000	40	4	CDEG
129	86	91	64	0.40	2.00	1.00	0.20	4.49	1000	60	4	CDEG
146	121	134	251	0.40	2.00	1.00	0.20	4.49	1000	100	4	CDEG
291	95	62	56	1.20	1.20	1.00	0.20	4.49	900	40	1	ADF
311	162	186	209	1.20	1.20	1.00	0.20	4.49	900	60	1	ADF
1314	238	271	155	1.20	1.20	1.00	0.20	4.49	900	100	1	ADF
764	286	180	229	2.00	2.00	0.20	0.20	3.39	900	40	2	ABCD
1759	723	930	262	2.00	2.00	0.20	0.20	3.39	900	60	2	ABCD
2497	1306	491	317	2.00	2.00	0.20	0.20	3.39	900	100	2	ABCD
339	96	103	124	1.20	1.20	1.00	0.20	4.69	900	40	3	ACF
696	107	183	138	1.20	1.20	1.00	0.20	4.69	900	60	3	ACF
1617	404	312	217	1.20	1.20	1.00	0.20	4.69	900	100	3	ACF
260	130	93	83	0.50	0.50	0.45	0.45	3.21	950	40	4	CP1
270	138	93	94	0.50	0.50	0.45	0.45	3.21	950	60	4	CP1
868	491	173	194	0.50	0.90	0.45	0.45	3.21	950	100	4	CP1
3768	2788	928	308	0.90	0.50	0.45	0.45	3.21	950	40	1	CP2
987	394	134	138	0.50	0.50	0.45	0.45	3.21	950	60	1	CP2
3198	11048	1849	1128	0.90	0.90	0.45	0.45	3.21	950	100	1	CP2
927	861	380	189	1.20	1.20	0.20	0.20	1.43	1000	40	2	BDG
940	923	490	156	1.20	1.20	0.20	0.20	1.43	1000	60	2	BDG
1192	1527	739	402	1.20	1.20	0.20	0.20	1.43	1000	100	2	BDG
546	68	79	76	1.20	1.20	0.20	1.00	4.80	900	40	3	ACF
7738	1159	629	988	1.20	1.20	0.20	1.00	4.80	900	60	3	ACF
13128	1368	2479	898	1.20	1.20	0.20	1.00	4.80	900	100	3	ACF
496	110	62	64	1.20	1.20	0.20	1.00	2.84	900	40	4	BDF
7318	888	309	728	1.20	1.20	0.20	1.00	2.84	900	60	4	BDF
1984	148	219	162	1.20	1.20	0.20	1.00	2.84	900	100	4	BDF
98	130	93	126	0.40	0.40	0.20	1.00	2.84	1000	40	1	FG
151	143	83	87	0.40	0.40	0.20	1.00	2.84	1000	60	1	FG
203	236	157	93	0.40	0.40	0.20	1.00	2.84	1000	100	1	FG
274	242	123	48	0.50	0.50	0.45	0.45	3.21	950	40	2	CP3
244	403	116	116	0.90	0.90	0.45	0.45	3.21	950	60	2	CP3
373	769	284	163	0.50	0.50	0.45	0.45	3.21	950	100	2	CP3
139	129	128	121	2.00	0.40	1.00	0.20	4.99	1000	40	3	ABEG
121	227	93	153	2.00	0.40	1.00	0.20	4.99	1000	60	3	ABEG
132	217	139	169	2.00	0.40	1.00	0.20	4.99	1000	100	3	ABEG
948	738	669	528	2.00	0.40	1.00	1.00	6.41	900	40	4	ABEF
437	55	58	44	2.00	0.40	1.00	1.00	6.41	900	60	4	ABEF
839	79	70	56	2.00	0.40	1.00	1.00	6.41	900	100	4	ABEF
591	632	145	127	2.00	2.00	0.20	1.00	4.80	1000	40	1	ABCDFG
1324	994	390	262	2.00	2.00	0.20	1.00	4.80	1000	60	1	ABCDFG
1545	1409	1105	728	2.00	2.00	0.20	1.00	4.80	1000	100	1	ABCDFG
248	67	46	74	0.40	0.40	0.20	0.20	1.43	900	40	2	(1)
461	678	69	99	0.40	0.40	0.20	0.20	1.43	900	60	2	(1)
2338	1068	2073	1349	0.40	0.40	0.20	0.20	1.43	900	100	2	(1)
1358	1918	429	858	0.50	0.50	0.45	0.45	3.21	950	40	3	CP4
156	878	96	117	0.50	0.50	0.45	0.45	3.21	950	60	3	CP4
366	363	315	150	0.50	0.50	0.45	0.45	3.21	950	100	3	CP4
144	146	108	96	1.20	1.20	1.00	1.00	6.41	1000	40	4	ADEFG
164	229	134	149	1.20	1.20	1.00	1.00	6.41	1000	60	4	ADEFG
230	292	191	163	1.20	1.20	1.00	1.00	6.41	1000	100	4	ADEFG
412	136	66	58	1.20	1.20	0.20	1.00	3.57	900	40	1	ACF
544	132	99	74	1.20	1.20	0.20	1.00	3.57	900	60	1	ACF
1132	156	90	150	1.20	1.20	0.20	1.00	3.57	900	100	1	ACF
900	951	307	113	1.20	1.20	0.20	0.20	2.15	1000	40	2	ACG
1718	944	382	186	1.20	1.20	0.20	0.20	2.15	1000	60	2	ACG
2740	1464	367	309	1.20	1.20	0.20	0.20	2.15	1000	100	2	ACG
357	468	219	133	2.00	2.00	1.00	0.20	5.72	1000	40	3	ABCDEG
461	606	277	127	2.00	2.00	1.00	0.20	5.72	1000	60	3	ABCDEG
912	785	926	186	2.00	2.00	1.00	0.20	5.72	1000	100	3	ABCDEG
1678	1948	678	369	1.20	1.20	1.00	1.00	5.17	1000	40	4	BDEFG
2308	1498	1544	678	1.20	1.20	1.00	1.00	5.17	1000	60	4	BDEFG
439	458	193	787	1.20	1.20	1.00	1.00	5.17	1000	100	4	BDEFG
699	130	103	139	0.40	2.00	0.20	0.20	2.15	900	40	1	CD
493	217	336	219	0.40	2.00	0.20	0.20	2.15	900	60	1	CD
1664	411	361	365	0.40	2.00	0.20	0.20	2.15	900	100	1	CD
378	268	112	146	2.00	0.40	0.20	1.00	4.08	1000	40	2	ABFG
344	682	109	1338	2.00	0.40	0.20	1.00	4.08	1000	60	2	ABFG
538	735	44	184	2.00	0.40	0.20	1.00	4.08	1000	100	2	ABFG
126	139	106	253	0.40	2.00	0.20	1.00	3.57	1000	40	3	CDFG
114	167	115	207	0.40	2.00	0.20	1.00	3.57	1000	60	3	CDFG
174	707	316	745	0.40	2.00	0.20	1.00	3.57	1000	100	3	CDFG
768	658	1104	888	1.20	1.20	1.00	0.20	5.72	900	40	4	ACF
316	137	144	135	1.20	1.20	1.00	0.20	5.72	900	40	4	ACE
1136	227	729	188	1.20	1.20	1.00	0.20	5.72	900	100	4	ACE

(1) Omitted, Second Pass.

TABLE III Continued.

[illegible]	[illegible]	[illegible]	[illegible]	[illegible]	[illegible]	[illegible]	[illegible]	[illegible]	TEMP	TIME	[illegible]	ID
[illegible] Y(.m)				ppm					(°C)	(hr)		
[illegible]	[illegible]	[illegible]	[illegible]	[illegible]	[illegible]	1.00	0.20	3.70	900	60	1	ADF
[illegible]	[illegible]	[illegible]	[illegible]	[illegible]	[illegible]	1.23	0.20	3.70	900	60	1	ADF
[illegible]	[illegible]	107	[illegible]	[illegible]	[illegible]	1.00	0.20	3.70	900	100	1	ADF
[illegible]	[illegible]	[illegible]	[illegible]	[illegible]	[illegible]	0.23	1.00	4.00	900	60	2	ADF
[illegible]	[illegible]	[illegible]	[illegible]	[illegible]	[illegible]	0.23	1.00	4.00	900	60	2	ADF
[illegible]	[illegible]	[illegible]	[illegible]	[illegible]	[illegible]	0.23	1.00	4.00	900	100	2	ADF
[illegible]	[illegible]	[illegible]	[illegible]	[illegible]	[illegible]	1.03	0.20	3.70	1000	60	3	FG
[illegible]	[illegible]	[illegible]	[illegible]	[illegible]	[illegible]	1.03	0.20	3.70	1000	60	3	FG
[illegible]	[illegible]	[illegible]	[illegible]	[illegible]	[illegible]	1.00	0.20	3.70	1000	100	3	FG
[illegible]	[illegible]	[illegible]	[illegible]	[illegible]	[illegible]	0.23	0.20	2.00	1000	60	4	ADG
[illegible]	[illegible]	[illegible]	[illegible]	[illegible]	[illegible]	0.23	0.20	2.00	1000	60	4	ADG
[illegible]	[illegible]	[illegible]	[illegible]	[illegible]	[illegible]	0.20	0.20	2.00	1000	100	4	ADG
[illegible]	[illegible]	[illegible]	[illegible]	[illegible]	[illegible]	[illegible]	0.20	2.00	900	60	1	AG
[illegible]	[illegible]	[illegible]	[illegible]	[illegible]	[illegible]	[illegible]	0.20	2.10	900	60	1	AG
[illegible]	[illegible]	[illegible]	[illegible]	[illegible]	[illegible]	[illegible]	0.20	2.10	900	100	1	AG
[illegible]	[illegible]	[illegible]	[illegible]	[illegible]	[illegible]	[illegible]	1.00	7.13	900	60	2	[illegible]
[illegible]	[illegible]	[illegible]	[illegible]	[illegible]	[illegible]	1.03	1.00	7.13	900	60	2	[illegible]
[illegible]	[illegible]	[illegible]	[illegible]	[illegible]	[illegible]	[illegible]	1.00	7.13	900	100	2	[illegible]
[illegible]	[illegible]	[illegible]	[illegible]	[illegible]	[illegible]	1.00	1.00	9.17	900	60	3	EF
[illegible]	[illegible]	[illegible]	[illegible]	[illegible]	[illegible]	1.00	1.00	9.17	900	60	3	EF
[illegible]	[illegible]	[illegible]	[illegible]	[illegible]	[illegible]	1.00	1.00	9.17	900	100	3	EF
[illegible]	[illegible]	[illegible]	[illegible]	[illegible]	[illegible]	1.00	1.00	7.13	1000	60	4	[illegible]
[illegible]	[illegible]	[illegible]	[illegible]	[illegible]	[illegible]	1.00	1.00	7.13	1000	60	4	[illegible]
[illegible]	[illegible]	[illegible]	[illegible]	[illegible]	[illegible]	1.00	1.00	7.13	1000	100	4	[illegible]
[illegible]	[illegible]	[illegible]	[illegible]	[illegible]	[illegible]	0.65	0.65	3.21	950	60	1	[illegible]
[illegible]	[illegible]	[illegible]	[illegible]	[illegible]	[illegible]	0.65	0.65	3.21	950	60	1	[illegible]
[illegible]	[illegible]	[illegible]	[illegible]	[illegible]	[illegible]	0.65	0.65	3.21	950	100	1	[illegible]
[illegible]	[illegible]	[illegible]	[illegible]	[illegible]	[illegible]	0.65	0.65	3.21	950	60	2	[illegible]
[illegible]	[illegible]	[illegible]	[illegible]	[illegible]	[illegible]	0.65	0.65	3.21	950	60	2	[illegible]
[illegible]	[illegible]	[illegible]	[illegible]	[illegible]	[illegible]	0.65	0.65	3.21	950	100	2	[illegible]
[illegible]	[illegible]	[illegible]	[illegible]	[illegible]	[illegible]	0.65	0.65	3.21	950	60	3	[illegible]
[illegible]	[illegible]	[illegible]	[illegible]	[illegible]	[illegible]	0.65	0.65	3.21	950	60	3	[illegible]
[illegible]	[illegible]	[illegible]	[illegible]	[illegible]	[illegible]	0.65	0.65	3.21	950	100	3	[illegible]
[illegible]	[illegible]	[illegible]	[illegible]	[illegible]	[illegible]	0.65	0.65	3.21	950	60	4	[illegible]
[illegible]	[illegible]	[illegible]	[illegible]	[illegible]	[illegible]	0.65	0.65	3.21	950	60	4	[illegible]
[illegible]	[illegible]	[illegible]	[illegible]	[illegible]	[illegible]	0.65	0.65	3.21	950	100	4	[illegible]
[illegible]	[illegible]	[illegible]	[illegible]	[illegible]	[illegible]	0.65	0.65	10.15	950	60	4	[illegible]
[illegible]	[illegible]	[illegible]	[illegible]	[illegible]	[illegible]	0.65	0.65	10.15	950	60	4	[illegible]
[illegible]	[illegible]	[illegible]	[illegible]	[illegible]	[illegible]	0.65	0.65	10.15	950	100	4	[illegible]
[illegible]	[illegible]	[illegible]	[illegible]	[illegible]	[illegible]	0.65	0.65	11.17	950	60	4	Fe
[illegible]	[illegible]	[illegible]	[illegible]	[illegible]	[illegible]	0.65	0.65	11.17	950	60	4	Fe
[illegible]	[illegible]	[illegible]	[illegible]	[illegible]	[illegible]	0.65	0.65	11.17	950	100	4	Fe
[illegible]	[illegible]	[illegible]	[illegible]	[illegible]	[illegible]	0.65	0.65	10.33	950	60	3	Fe
[illegible]	[illegible]	[illegible]	[illegible]	[illegible]	[illegible]	0.65	0.65	10.33	950	60	3	Fe
[illegible]	[illegible]	[illegible]	[illegible]	[illegible]	[illegible]	0.65	0.65	10.33	950	100	3	Fe
[illegible]	[illegible]	[illegible]	[illegible]	[illegible]	[illegible]	0.65	0.65	3.21	950	60	3	CPSTAR1
[illegible]	[illegible]	[illegible]	[illegible]	[illegible]	[illegible]	0.65	0.65	3.21	950	60	3	CPSTAR1
[illegible]	[illegible]	[illegible]	[illegible]	[illegible]	[illegible]	0.65	0.65	3.21	950	100	3	CPSTAR1
[illegible]	[illegible]	[illegible]	[illegible]	[illegible]	[illegible]	0.65	0.65	3.21	950	60	3	B-
[illegible]	[illegible]	[illegible]	[illegible]	[illegible]	[illegible]	0.65	0.65	3.21	950	60	3	B-
[illegible]	[illegible]	[illegible]	[illegible]	[illegible]	[illegible]	0.65	0.65	3.21	950	100	3	B-
[illegible]	[illegible]	[illegible]	[illegible]	[illegible]	[illegible]	0.65	0.65	7.29	950	60	4	Co
[illegible]	[illegible]	[illegible]	[illegible]	[illegible]	[illegible]	0.65	0.65	7.29	950	60	4	Co
[illegible]	[illegible]	[illegible]	[illegible]	[illegible]	[illegible]	0.65	0.65	7.29	950	100	4	Co
[illegible]	[illegible]	[illegible]	[illegible]	[illegible]	[illegible]	0.65	[illegible]	2.04	950	60	3	F-
[illegible]	[illegible]	[illegible]	[illegible]	[illegible]	[illegible]	0.65	[illegible]	2.04	950	60	3	F-
[illegible]	[illegible]	[illegible]	[illegible]	[illegible]	[illegible]	0.65	0.04	2.04	950	100	3	F-
[illegible]	[illegible]	[illegible]	[illegible]	[illegible]	[illegible]	0.65	0.65	3.21	800	60	3	G-
[illegible]	[illegible]	[illegible]	[illegible]	[illegible]	[illegible]	0.65	0.65	3.21	800	60	3	G-
[illegible]	[illegible]	[illegible]	[illegible]	[illegible]	[illegible]	0.65	0.65	3.21	800	100	3	G-
[illegible]	[illegible]	[illegible]	[illegible]	[illegible]	[illegible]	0.65	0.65	3.21	1100	60	4	Ge
[illegible]	[illegible]	[illegible]	[illegible]	[illegible]	[illegible]	0.65	0.65	3.21	1100	60	4	Ge
[illegible]	[illegible]	[illegible]	[illegible]	[illegible]	[illegible]	0.65	0.65	3.21	1100	100	4	Ge
[illegible]	[illegible]	[illegible]	[illegible]	[illegible]	[illegible]	0.65	0.65	3.21	950	60	4	CPSTAR2
[illegible]	[illegible]	[illegible]	[illegible]	[illegible]	[illegible]	0.65	0.65	3.21	950	60	4	CPSTAR2
[illegible]	[illegible]	[illegible]	[illegible]	[illegible]	[illegible]	0.65	0.65	3.21	950	100	4	CPSTAR2
[illegible]	[illegible]	[illegible]	[illegible]	[illegible]	[illegible]	0.65	0.65	3.21	950	60	3	De
[illegible]	[illegible]	[illegible]	[illegible]	[illegible]	[illegible]	0.65	0.65	3.21	950	60	3	De
[illegible]	[illegible]	[illegible]	[illegible]	[illegible]	[illegible]	0.65	0.65	3.21	950	100	3	De
[illegible]	[illegible]	[illegible]	[illegible]	[illegible]	[illegible]	[illegible]	0.65	2.01	950	60	4	F-
[illegible]	[illegible]	[illegible]	[illegible]	[illegible]	[illegible]	[illegible]	0.65	2.01	950	60	4	F-
[illegible]	[illegible]	[illegible]	[illegible]	[illegible]	[illegible]	[illegible]	0.65	2.01	950	100	4	F-
[illegible]	[illegible]	[illegible]	[illegible]	[illegible]	[illegible]	0.65	0.65	2.58	950	60	3	A-
[illegible]	[illegible]	[illegible]	[illegible]	[illegible]	[illegible]	0.65	0.65	2.58	950	60	3	A-
[illegible]	[illegible]	[illegible]	[illegible]	[illegible]	[illegible]	0.65	0.65	2.58	950	100	3	A-
[illegible]	[illegible]	[illegible]	[illegible]	[illegible]	[illegible]	0.65	0.65	2.84	950	60	4	C-
[illegible]	[illegible]	[illegible]	[illegible]	[illegible]	[illegible]	0.65	0.65	2.84	950	60	4	C-
[illegible]	[illegible]	[illegible]	[illegible]	[illegible]	[illegible]	0.65	0.65	2.84	950	100	4	C-
[illegible]	[illegible]	[illegible]	[illegible]	[illegible]	[illegible]	0.65	0.65	3.21	950	60	4	Be
[illegible]	[illegible]	[illegible]	[illegible]	[illegible]	[illegible]	0.65	0.65	3.21	950	60	4	Be
[illegible]	[illegible]	[illegible]	[illegible]	[illegible]	[illegible]	0.65	0.65	3.21	950	100	4	Be
[illegible]	[illegible]	[illegible]	[illegible]	[illegible]	[illegible]	0.65	0.65	3.21	950	60	3	D-
[illegible]	[illegible]	[illegible]	[illegible]	[illegible]	[illegible]	0.65	0.65	3.21	950	60	3	D-
[illegible]	[illegible]	[illegible]	[illegible]	[illegible]	[illegible]	0.65	0.65	3.21	950	100	3	D-
[illegible]	[illegible]	[illegible]	[illegible]	[illegible]	[illegible]	1.00	0.20	4.55	900	60	3	ADF-2
[illegible]	[illegible]	[illegible]	[illegible]	[illegible]	[illegible]	1.00	0.20	4.55	900	60	3	ADF-2
[illegible]	[illegible]	[illegible]	[illegible]	[illegible]	[illegible]	1.00	0.20	4.59	900	100	3	ADF-2
[illegible]	[illegible]	[illegible]	[illegible]	[illegible]	[illegible]	1.00	0.20	4.72	900	60	4	ACF-2
[illegible]	[illegible]	[illegible]	[illegible]	[illegible]	[illegible]	1.00	0.20	4.72	900	60	4	ACF-2
[illegible]	[illegible]	[illegible]	[illegible]	[illegible]	[illegible]	1.00	0.20	4.72	900	100	4	ACF-2
[illegible]	[illegible]	[illegible]	[illegible]	[illegible]	[illegible]	0.23	0.20	1.43	900	60	3	D
[illegible]	[illegible]	[illegible]	[illegible]	[illegible]	[illegible]	0.23	0.20	1.43	900	60	3	D
[illegible]	[illegible]	[illegible]	[illegible]	[illegible]	[illegible]	0.23	0.20	1.43	900	100	3	D
[illegible]	[illegible]	[illegible]	[illegible]	1.20	2.00	0.20	1.00	4.80	900	60	4	ACDF
[illegible]	[illegible]	[illegible]	[illegible]	1.20	2.00	0.20	1.00	4.80	900	60	4	ACDF
[illegible]	[illegible]	[illegible]	[illegible]	1.20	2.00	0.20	1.00	4.80	900	100	4	ACDF

(1) Omitted, First Pass.

TABLE III. - Concluded.

	τ(μm)					ppm			(°C)	(hr)		
IN100	U700	IN792	MM200	NA	[illegible]	MG	CA	CL	TEMP	TIME	FIG	ID
669	80	105	91	0.60	1.20	0.20	0.20	2.15	900	40	3	C
848	93	233	166	0.60	1.20	0.20	0.20	2.15	900	60	3	C
16.4	201	203	247	0.60	1.20	0.20	0.20	2.15	900	100	3	C
119	70	98	43	1.20	0.40	0.20	1.00	4.00	900	40	4	AF
307	70	468	218	1.20	0.40	0.20	1.00	4.00	900	60	4	AF
1223	108	30	91	1.20	0.40	0.20	1.00	4.00	900	100	4	AF
2626	808	779	1098	1.20	0.40	1.00	0.20	3.76	900	40	3	BF
4100	988	1179	1088	1.20	0.40	1.00	0.20	3.76	900	60	3	BF
[illegible]	[illegible]	1610	[illegible]	1.20	0.40	1.00	0.20	3.76	900	100	3	BF
69	93	56	66	2.00	1.20	1.00	1.00	7.13	900	40	4	ABCEF
169	92	52	54	2.00	1.20	1.00	1.00	7.13	900	60	4	ABCEF
990	86	87	99	2.00	1.20	1.00	1.00	7.13	900	100	4	ABCEF
596	636	209	190	2.00	1.20	0.20	1.00	4.08	1000	40	3	ABDFG
910	793	359	122	2.00	1.20	0.20	1.00	4.08	1000	60	3	ABDFG
1177	1541	681	346	2.00	1.20	0.20	1.00	4.08	1000	100	3	ABDFG
681	417	331	119	1.20	2.00	0.20	0.20	2.15	1000	40	4	BCDG
833	567	366	155	1.20	2.00	0.20	0.20	2.15	1000	60	4	BCDG
1251	963	526	401	1.20	2.00	0.20	0.20	2.15	1000	100	4	BCDG
86	87	65	97	0.90	0.90	0.45	0.45	3.21	950	40	4	CPIFLSI1
240	196	92	129	0.90	0.90	0.45	0.45	3.21	950	60	4	CPIFLSI1
[illegible]	387	116	116	0.90	0.90	0.45	0.45	3.21	950	100	4	CPIFLSI1
161	101	77	91	0.90	0.90	0.45	0.45	3.21	950	40	3	CPIFLSI2
217	209	93	85	0.90	0.90	0.45	0.45	3.21	950	60	3	CPIFLSI2
300	230	116	191	0.90	0.90	0.45	0.45	3.21	950	100	3	CPIFLSI2
606	82	59	79	0.90	1.23	1.26	0.09	0.46	900	40	3	EXPAND 1
909	155	88	188	0.90	1.23	1.26	0.09	0.46	900	60	3	EXPAND 1
[illegible]	[illegible]	1676	[illegible]	0.90	1.23	1.26	0.09	0.46	900	100	3	EXPAND 1
972	442	366	271	1.90	3.90	1.00	0.79	0.00	900	40	4	EXPAND 3
1613	630	565	329	1.90	3.90	1.00	0.79	0.00	900	60	4	EXPAND 3
2677	1831	817	473	1.90	3.90	1.00	0.79	0.00	900	100	4	EXPAND 3
361	116	62	163	1.90	0.90	1.54	0.79	0.46	900	40	3	EXPAND 4
962	203	88	131	1.90	0.90	1.54	0.79	0.46	900	60	3	EXPAND 4
[illegible]	[illegible]	101	252	1.90	0.90	1.54	0.79	0.46	900	100	3	EXPAND 4
6670	2200	1600	1050	4.70	1.90	0.93	0.63	0.00	900	40	4	EXPAND 7
1360	1077	337	218	4.70	1.90	0.93	0.63	0.00	900	60	4	EXPAND 7
1969	1952	750	209	4.70	1.90	0.93	0.63	0.00	900	100	4	EXPAND 7
128	96	66	77	0.90	1.23	1.26	0.09	0.46	1000	40	3	EXPAND 2
179	309	173	81	0.90	1.23	1.26	0.09	0.46	1000	60	3	EXPAND 2
266	[illegible]	[illegible]	140	0.90	1.23	1.26	0.09	0.46	1000	100	3	EXPAND 2
1593	721	415	319	1.90	3.90	1.00	0.79	0.00	1000	40	4	EXPAND 5
2123	1002	551	301	1.90	3.90	1.00	0.79	0.00	1000	60	4	EXPAND 5
3716	1095	424	400	1.90	3.90	1.00	0.79	0.00	1000	100	4	EXPAND 5
635	637	160	98	1.90	0.90	1.54	0.79	0.46	1000	40	3	EXPAND 6
822	[illegible]	317	321	1.90	0.90	1.54	0.79	0.46	1000	60	3	EXPAND 6
1522	[illegible]	425	[illegible]	1.90	0.90	1.54	0.79	0.46	1000	100	3	EXPAND 6
1730	1017	560	300	4.70	1.90	0.93	0.63	0.00	1000	40	4	EXPAND 8
2694	1749	780	476	4.70	1.90	0.93	0.63	0.00	1000	60	4	EXPAND 8
4194	2943	1384	603	4.70	1.90	0.93	0.63	0.00	1000	100	4	EXPAND 8
28	26	36	20	0.00	0.00	0.00	0.00	0.00	900	40	4	OXIDAT
25	19	28	38	0.00	0.00	0.00	0.00	0.00	900	60	4	OXIDAT
-999(3)	74	29	79	0.00	0.00	0.00	0.00	0.00	900	100	4	OXIDAT
67	67	155	150	0.00	0.00	0.00	0.00	0.00	1100	40	1	OXIDAT
43	88	175	201	0.00	0.00	0.00	0.00	0.00	1100	60	1	OXIDAT
74	78	259	294	0.00	0.00	0.00	0.00	0.00	1100	100	1	OXIDAT
62	97	72	72	0.00	0.00	0.00	0.00	0.00	1000	40	2	OXIDAT
-999	26	72	-999	0.00	0.00	0.00	0.00	0.00	1000	60	2	OXIDAT
56	94	101	112	0.00	0.00	0.00	0.00	0.00	1000	100	2	OXIDAT
51	-999	66	62	0.00	0.00	0.00	0.00	0.00	950	40	3	OXIDAT
61	-999	59	47	0.00	0.00	0.00	0.00	0.00	950	60	3	OXIDAT
17	-999	44	137	0.00	0.00	0.00	0.00	0.00	950	100	3	OXIDAT
450	737	161	193	0.90	0.90	0.45	0.45	3.21	950	80	1	CPD
362	637	177	117	0.90	0.90	0.45	0.45	3.21	950	80	2	CPD
415	471	161	51	0.90	0.90	0.45	0.45	3.21	950	80	3	CPD
314	503	218	78	0.90	0.90	0.45	0.45	3.21	950	80	4	CPD
1309	2066	931	233	0.90	0.90	0.45	0.45	3.21	950	200	1	CPFND
1023	1190	603	177	0.90	0.90	0.45	0.45	3.21	950	200	2	CPFND
544	770	275	174	0.90	0.90	0.45	0.45	3.21	950	200	3	CPFND
702	928	366	164	0.90	0.90	0.45	0.45	3.21	950	200	4	CPFND

(3) Omitted, Negative τ

ORIGINAL PAGE IS
OF POOR QUALITY

TABLE IV. - CENTER POINT REGRESSION ANALYSES (56 DATA POINTS PER ALLOY)

	IN-100			U-700			IN-792			MM 509		
	EST COEF	STD DEV COEF	t	EST COEF	STD DEV COEF	t	EST COEF	STD DEV COEF	t	EST COEF	STD DEV COEF	t
β_0	1.032			.631			.715			1.420		
log (time)	.98	.082	12.04	1.36	.132	10.36	.87	.082	10.61	.60	.099	6.02
F/A	$-.67\times10^{-3}$	$.25\times10^{-3}$	-2.69	-1.22×10^{-3}	$.40\times10^{-3}$	-3.02	$-.30\times10^{-3}$	$.25\times10^{-3}$	-1.21	$-.96\times10^{-3}$	$.3\times10^{-3}$	-3.15
r_1	-.11	.016	-6.97	-.14	.026	-5.39	-.068	.016	-4.16	-.006	.020	-.29
r_2	$.26\times10^{-2}$	.015	.16	6.1×10^{-2}	.026	2.31	1.99×10^{-2}	.016	1.22	2.9×10^{-2}	.020	1.45
r_1r_2	$.56\times10^{-1}$	.018	3.17	$.41\times10^{-1}$	.028	1.44	$-.16\times10^{-1}$	.018	-.89	$-.26\times10^{-1}$	.021	-1.24
R^2		82.1			76.5			73.6			45.7	
$\hat{\sigma}^2$	.0099	.0142	.0219	.0257	.0367	.0568	.0099	.0141	.0219	.0146	.0209	.0323
$\hat{\sigma}$		.119			.192			.119			.145	
$10^{\pm 2\hat{\sigma}}$	.58		1.73	.41		2.42	.58		1.73	.57		1.95

TABLE V. - RESULTS OF MODEL FITTED BY DROPPING POINTS LABELED (a) AND (b) IN TABLE III

	IN-100		U-700		IN-792		MarM-509	
	$\hat{\alpha}_1$	$\hat{\alpha}_2$	$\hat{\alpha}_1$	$\hat{\alpha}_2$	$\hat{\alpha}_1$	$\hat{\alpha}_2$	$\hat{\alpha}_1$	$\hat{\alpha}_2$
Na	336.4	.07666	105.2	.06592	259.4	.007793	2.667	.2838
K	90.66	.01373	13.10	.1801	15.77	.1606	8.384	.1166
Mg	.4661	2.039	.7399	1.009	.5489	2.598	2.773	.02431
Cl	.2312	.5443	.2430	.354[illegible]	.4104	.5023	.1856	.1334
Ca	.4345	0.000	.6070	.7410	.1953	.9624	.4914	.2500
γ log t	.9950		1.062		.8218		.6515	
β	-.08192		-.4103		.3137		.6720	
βT	-.1234		.1870		.1227		.05306	
βT^2	.04424		-.05006		-.004882		.02438	
βr_1	-.05016		-.09450		-.05501		-.02612	
βr_2	-.02319		.01082		-.03358		-.02606	
βr_1r_2	.01950		.007929		.005913		.001433	
SSQ TOT	44.54		44.06		25.01		13.23	
SSQ RES	7.19		7.53		4.23		3.86	
R^2	.839		.829		.831		.708	
n	203		200		205		203	
$\hat{\sigma}^2$	.0387		.0411		.0225		.0208	
$\hat{\sigma}$	.197		.203		.150		.144	
$10^{\pm 2\hat{\sigma}}$	(.404 , 2.47)		(.393 , 2.55)		(.501 , 1.99)		(.515 , 1.94)	

TABLE VI. - ESTIMATED RIG VARIATION FROM NOMINAL ($r_1=0$, $r_2=0$)

Dummy Variables		Rig No.	$10^{\beta r_1 + \beta r_2 + \beta r_1 r_2}$			
r_1	r_2		IN-100	U-700	IN-792	MM 509
-1	-1	1	1.24	1.23	1.24	1.13
-1	+1	2	1.02	1.25	1.04	1.00
+1	-1	3	.90	.77	.94	1.00
+1	+1	4	.88	.84	.83	.89

TABLE VII. - PHASES PRESENT IN DEPOSITS

R.O.

DATE

RUN CODE	No.	Dopant Composition (ppm) Na	K	Mg	Ca	Cl	Temp. (°C)	Phases Present (Relative Strength of X-Ray Diffraction Patterns; s = strong, m = medium, w = weak) MgO	$NaSO_4$	$CaSO_4$	$K_xNa_{(2-x)}SO_4$	$Na_8Ca_2K_1SO_4$ (1)	Substrate Oxides (2)	Other Known Phases	Unknown Pattern
Center Points	All	0.90	0.90	0.45	0.45	3.21	950	S	M	M		M	W		
A$^+$	4	5.49	0.90	0.45	0.45	10.35	950	M	S						
AB	1	2.00	0.40	0.20	0.20	2.66	900	M	S				W		
A$^-$	3	0.49	0.90	0.45	0.45	2.58	950	M		S					
B$^+$	4	5.49	0.90	0.45	0.45	5.21	950	M	S						
B$^-$	3	0.49	0.90	0.45	0.45	3.21	950	M		S					
C$^+$	4	0.90	5.40	0.45	0.45	7.29	950	S			S				
C	3	0.49	1.20	0.20	0.20	2.15	900	S			S	M	W		
CD	1	0.49	2.00	0.20	0.20	2.15	900	S			S				
C$^-$	4	0.90	0.49	0.45	0.45	2.84	950	S		M		S			W
D$^+$	3	0.90	5.40	0.45	0.45	3.12	950	S			S				
D	3	0.40	1.20	0.20	0.20	1.43	900	S			S	M	M		
D$^-$	3	0.90	0.49	0.45	0.45	3.21	950	S		S		S			
E$^+$	3	0.90	0.90	4.95	0.45	16.33	950	S		M			W		
EG	3	0.40	0.40	1.00	0.20	3.76	1000	S		S					
E$^-$	4	0.90	0.90	0.04	0.45	2.01	950					S	S		
F$^+$	4	0.90	0.90	0.45	4.95	11.17	950	W		S					
FG	1	0.40	0.40	0.20	1.00	2.84	1000	S		S					
F$^-$	3	0.90	0.90	0.45	0.04	2.48	950		S				S		
EF	3	0.40	0.40	1.00	1.00	5.17	900	S		S			M		
G$^+$	4	0.90	0.90	0.45	0.45	3.21	1100	S				S			
G$^-$	3	0.90	0.90	0.45	0.45	3.21	800	S				S			
ACG	3	1.20	1.20	0.20	0.20	3.39	1000		M		W		S		
ADG	4	1.20	1.20	0.20	0.20	2.66	1000	W	M		M		S		
BCG	2	1.20	1.20	0.20	0.20	2.15	1000		M		W		S		W
BDG	2	1.20	1.20	0.20	0.20	1.43	1000		S	W	W		S		W

NASA-C-8017 (10-24-51)

(1) See text of Appendix fc. discussion of this phase.

(2) Substrate oxides usually strongest on IN-100 samples.

TABLE VII. - Continued.

R.O.

DATE

RUN CODE	RIG	Dopant Composition (ppm) Na	K	Mg	Ca	Cl	Temp. (°C)	Phases Present (Relative Strength of X-Ray Diffraction Patterns) S = strong, M = medium, W = weak MgO	NaSO$_4$	CaSO$_4$	K Mg (2:x) SO$_4$	Na$_8$Ca$_2$K$_1$ SO$_4$	Substrate Oxides	Other Known Phases	Unknown Pattern
ABCD	2	2.00	2.00	0.20	0.20	3.39	900	M	S		S	M	S		M
BCDG	4	1.20	2.00	0.20	0.20	2.15	1000	M			S		S		
BE	3	1.20	0.40	1.00	0.20	3.76	900	S	S			S			
ABEG	3	2.00	0.40	1.00	0.20	4.99	1000	S	M						M
ADE-I	1	1.20	1.20	1.00	0.20	4.99	900	S	M	M	M				M
ADE-II	3	1.20	1.20	1.00	0.20	4.99	900	S	S					(W) Na$_2$CaSO$_4$	
ACE-I	4	1.20	1.20	1.00	0.20	5.72	900	S	M		M				
ACE-II	4	1.20	1.20	1.00	0.20	5.72	900	S			M	M			
BCE	3	1.20	1.20	1.00	0.20	4.49	900	S	M		M				
BDE	1	1.20	1.20	1.00	0.20	3.76	900	S	M		M				
ABCDEG	3	2.00	2.00	1.00	0.20	5.72	1000	S	M		M		M		
CDEG	4	0.40	2.00	1.00	0.20	4.49	1000	M		M	M				
ABFG	2	2.00	0.40	0.20	1.00	4.08	1000					S	M		
AF	4	1.20	0.40	0.20	1.00	4.08	900	M		M		S			
ACF	3	1.20	1.20	0.20	1.00	4.80	900	M	S	M					M
ADF	2	1.20	1.20	0.20	1.00	4.08	900	S		S		S			M
BCF	1	1.20	1.20	0.20	1.00	3.57	900	S		S	M	S			M
BDF	4	1.20	1.20	0.20	1.00	2.94	900	S	S	S					M
ACDF	4	1.20	2.00	0.20	1.00	4.80	900	S				S		K$_2$Ca$_2$(SO$_4$)$_3$	
ABDFG	2	2.00	1.20	0.20	1.00	4.08	1000		M			S			M
ABCDFG	1	2.00	2.00	0.20	1.00	4.80	1000		S				M		
CDFG	3	0.40	2.00	0.20	1.00	3.57	1000			S			M		
ABEF	3	2.00	0.40	1.00	1.00	6.41	900	S		M					M
ABCEF	4	2.00	1.20	1.00	1.00	7.13	900	S		M		S			M
ABCDEF	2	2.00	2.00	1.00	1.00	7.13	900	S		S		S	M		M
ACEFG	4	1.20	1.20	1.00	1.00	7.13	1000	S	M	S					

TABLE VII. - Concluded.

RUN CODE	RIG	Dopant Composition (ppm) Na	K	Mg	Ca	Cl	Temp. (°C)	Phases Present (Relative Strength of X-Ray Diffraction Patterns) s = strong, m = medium, w = weak MgO	$NaSO_4$	$CaSO_4$	$K_xNa_{(2-x)}SO_4$	$Na_6Ca_2K_1SO_4$	Substrate Oxides	Other Known Phases	Unknown Pattern
ADEFG	4	1.20	1.20	1.00	1.00	6.41	1000	S		S					
BDEFG	4	1.20	1.20	1.00	1.00	5.17	1000	S		S					
BCEFG	1	1.20	1.20	1.00	1.00	5.90	1000	S		S			W		
CDEF	2	0.40	2.00	1.00	1.00	5.90	900	S		S					
(L)	2	0.40	0.40	0.20	0.20	1.43	900	S			M		S		M
1	3	0.58	1.23	1.26	0.95	0.46	900	M			M		S	$K_2Ca_2(SO_4)_3$	
2	3	0.58	1.23	1.26	0.95	0.46	1000			M			S		
3	4	1.50	3.90	1.00	0.75	0.60	900	M			S				M
4	4	1.50	3.90	1.00	0.75	0.60	1000				M		S		
5	3	1.90	0.50	1.05	0.79	0.48	900	S					S		M
6	3	1.90	0.50	1.05	0.79	0.48	1000	S					S		M
7	4	4.70	1.50	0.83	0.63	0.60	900	M	S		M				
8	4	4.70	1.50	0.83	0.63	0.60	1000	M	S		M				

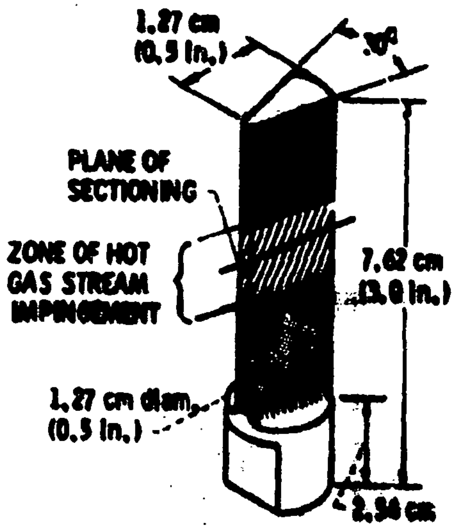

(a) TEST BAR.

(b) BURNER RIG.

Figure 1. - Hot-corrosion apparatus and test specimen.

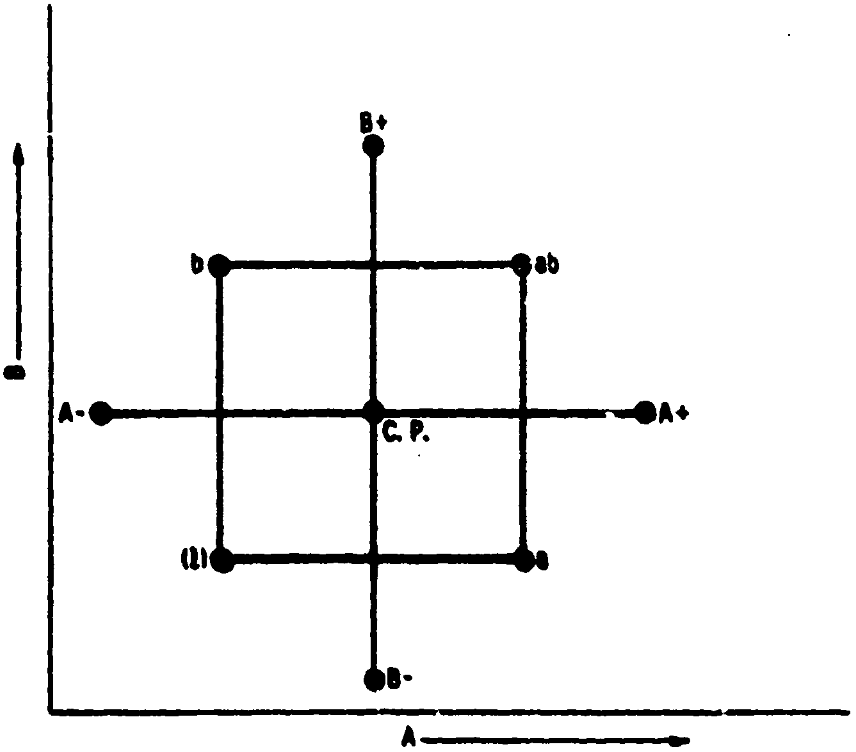

Figure 2. - A central composite factorial design for two variables, A and B. A± and B± denote axial or star points; C. P. denotes a center point; and a, b, ab, and (1) denote cube points.

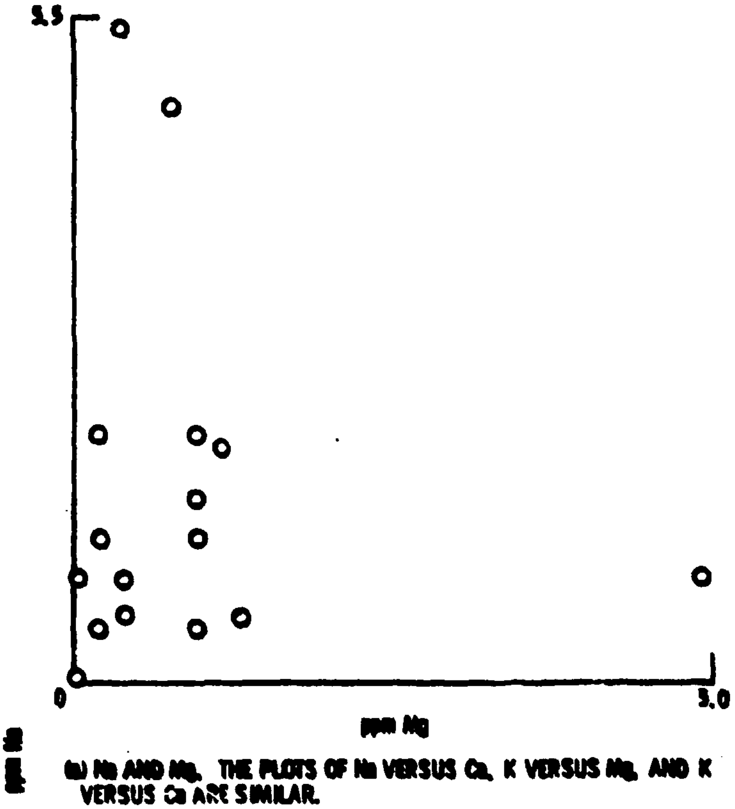

(a) Na AND Mg. THE PLOTS OF Na VERSUS Ca, K VERSUS Mg, AND K VERSUS Ca ARE SIMILAR.

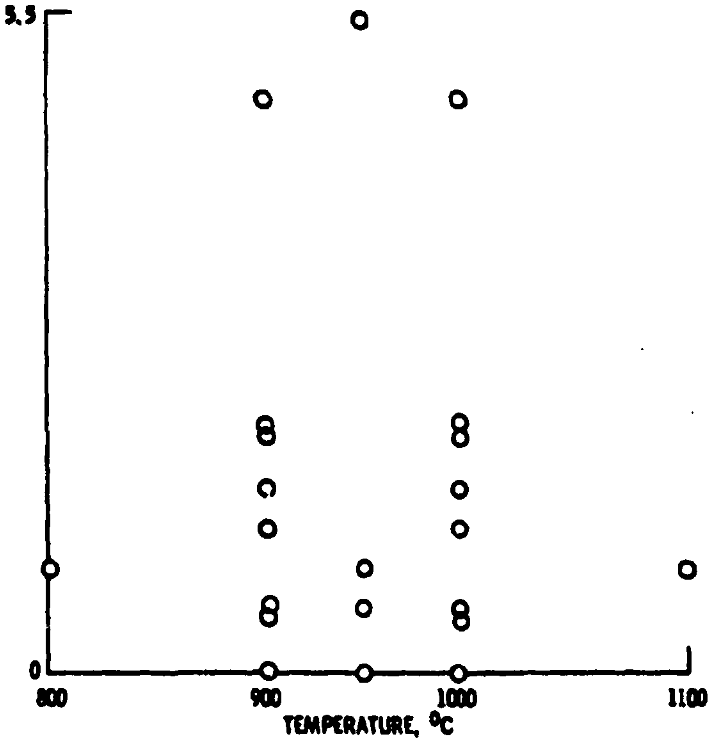

(b) TEMPERATURE AND Na. THE PLOT OF K VERSUS T IS SIMILAR.

Figure 3. - The scope of the program.

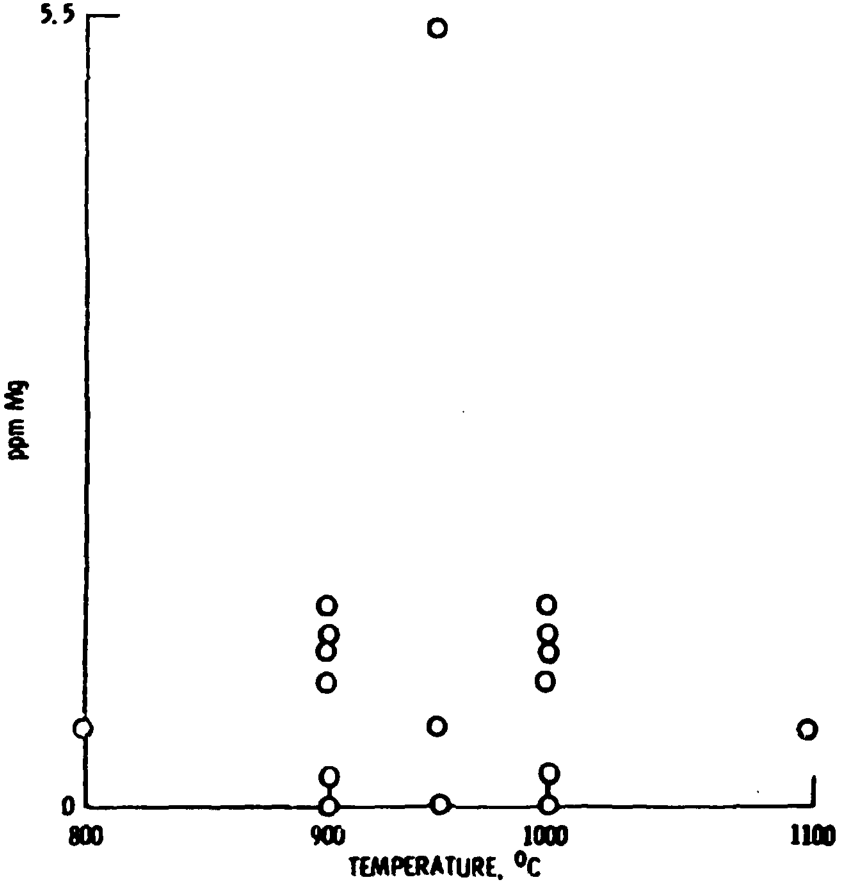

(c) TEMPERATURE AND Mg. THE PLOT OF Ca VERSUS T IS SIMILAR.

Figure 3. - Concluded.

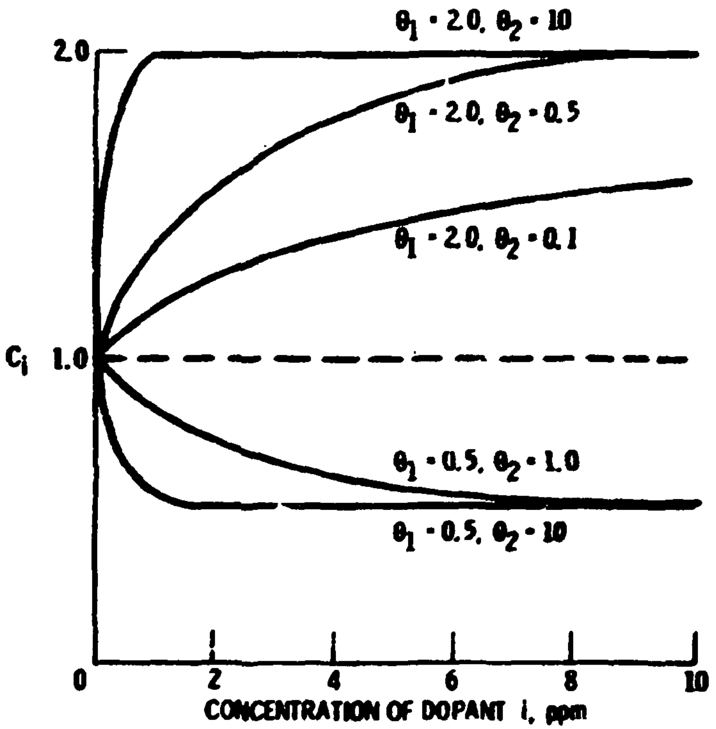

Figure 4. - The response of C_i to concentration of dopant "i" as affected by variations in φ_1 and φ_2.

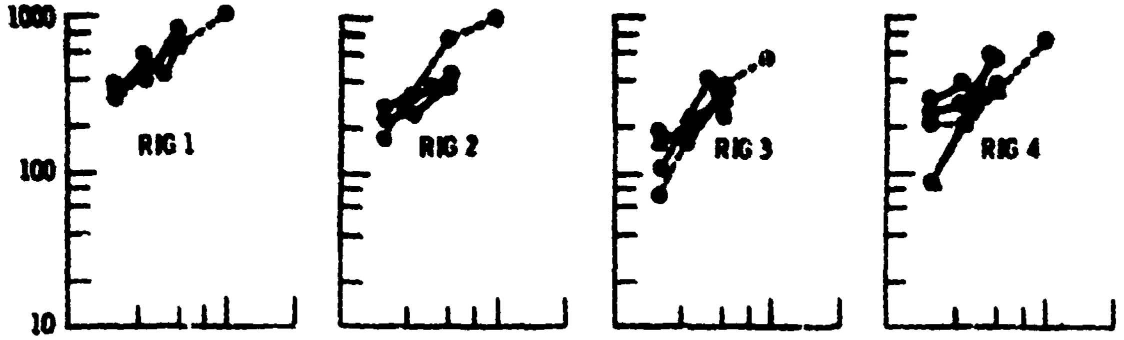

(a) IN-100.

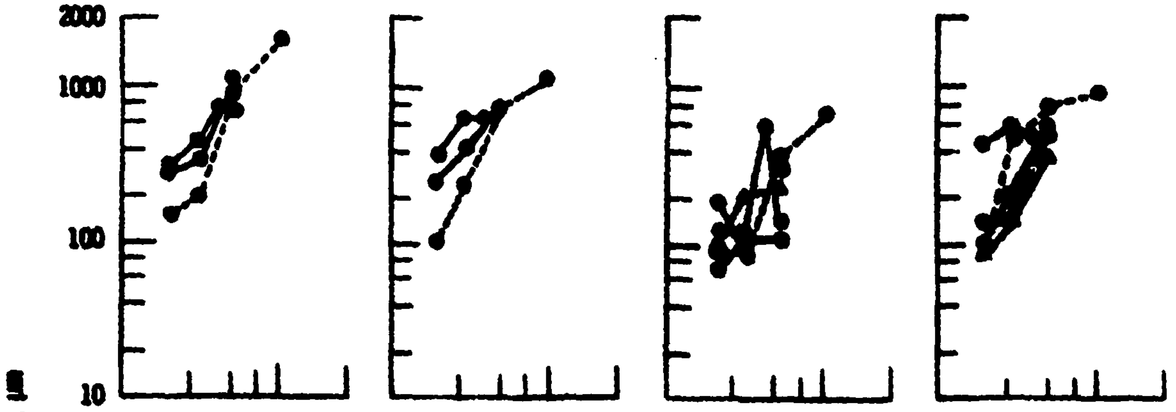

(b) U-700.

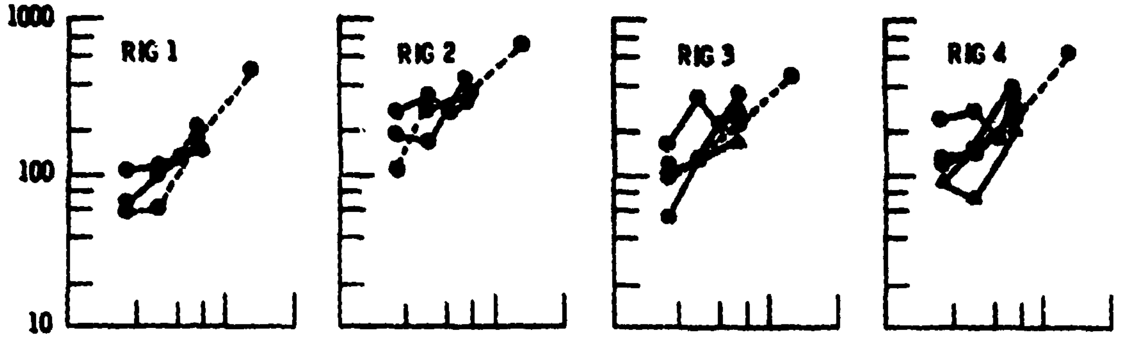

(c) IN-792.

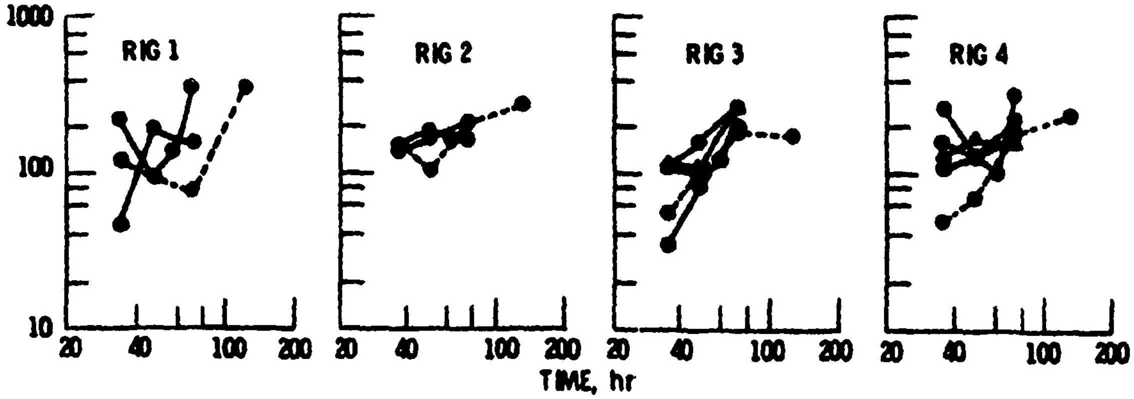

(d) MAR M-509.

Figure 5. - Effects of rig and time on the center point metal recession.

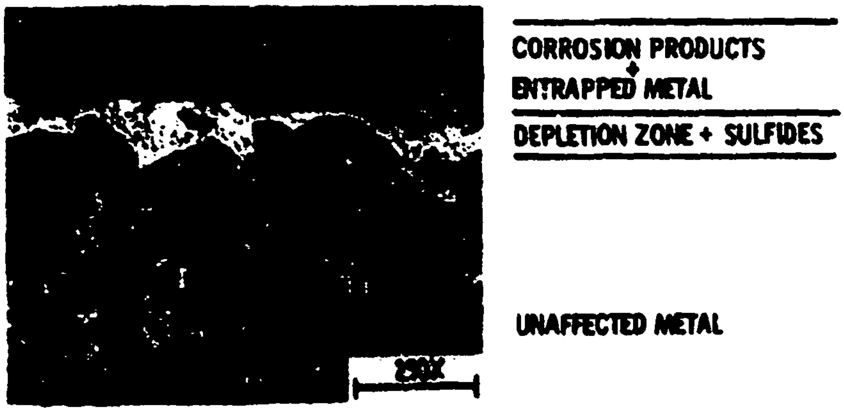

(a) IN-100.

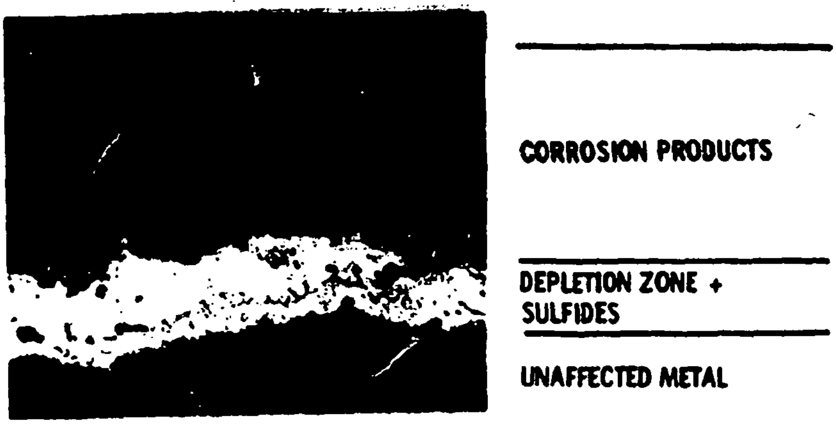

(b) U-700.

Figure 6. - Microstructural attack after 200 one-Hour cycles under center point conditions. (950°C, 0.90Na, 0.9K, 0.45Ca, 0.45Mg, 3.21Cl)

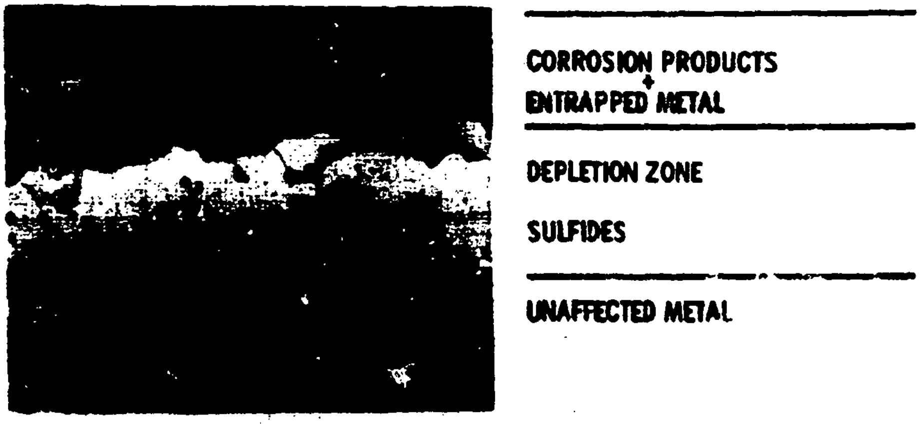

(c) IN-792

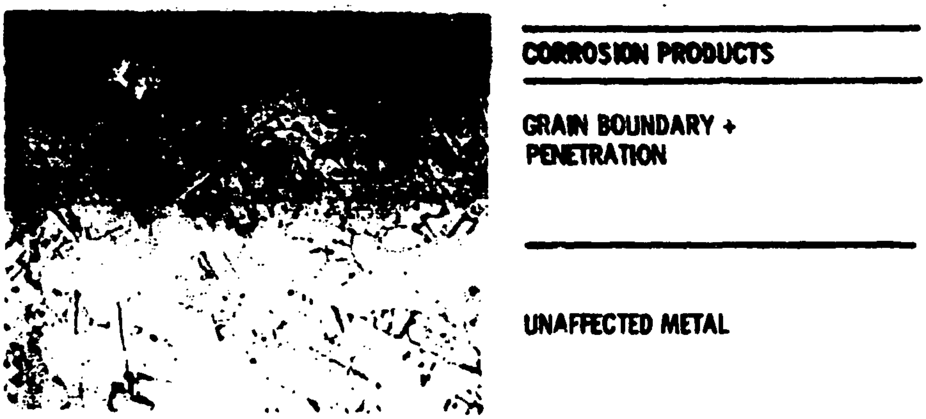

MAR M-509

Figure 6. - Concluded.

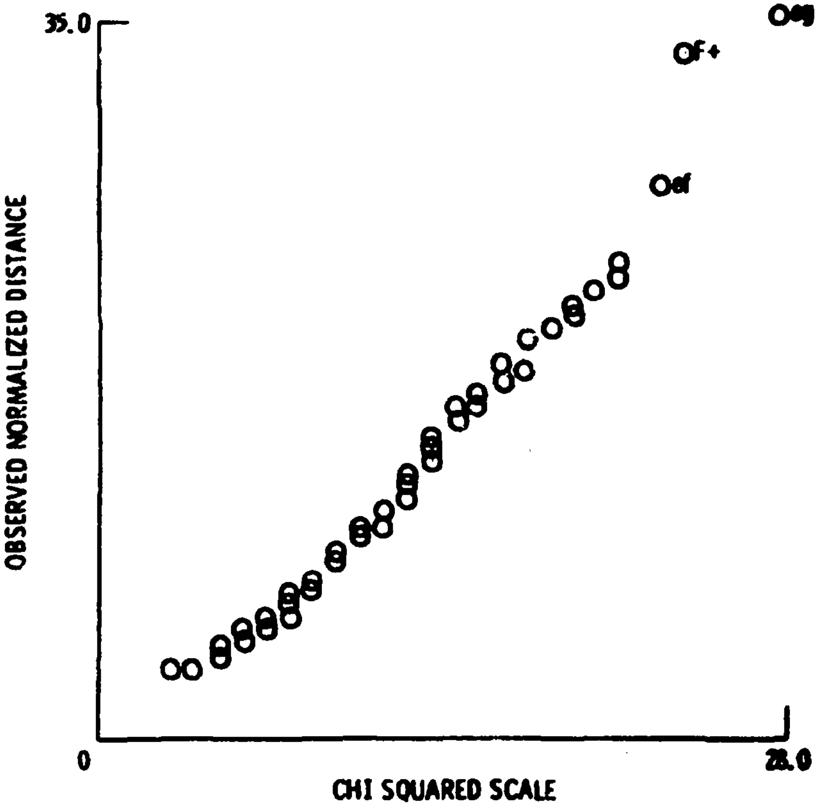

Figure 7. - Probability plot of pass 1 residuals.

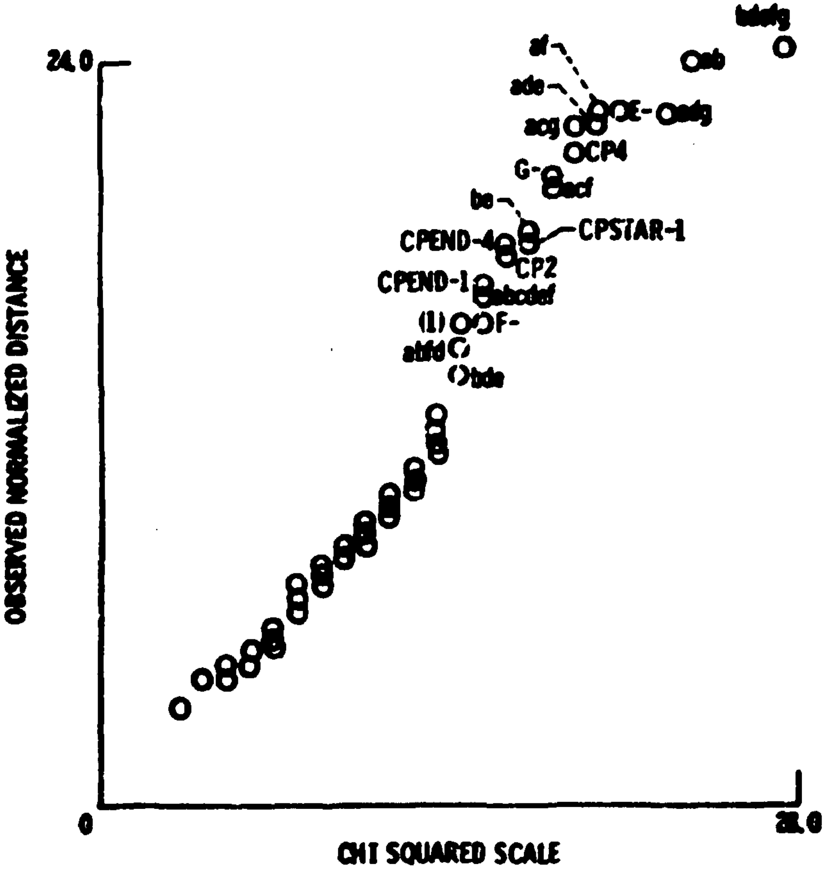

Figure 8. - Probability plot of pass 2 residuals.

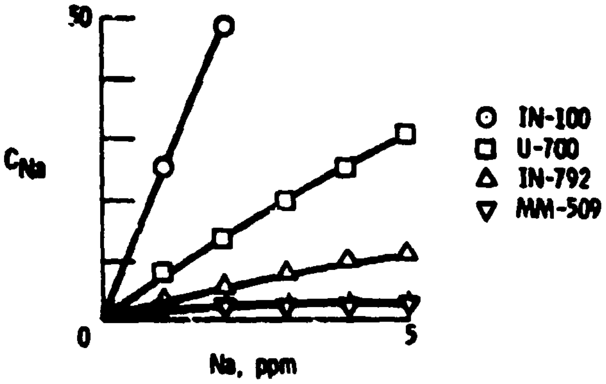

(a) SODIUM.

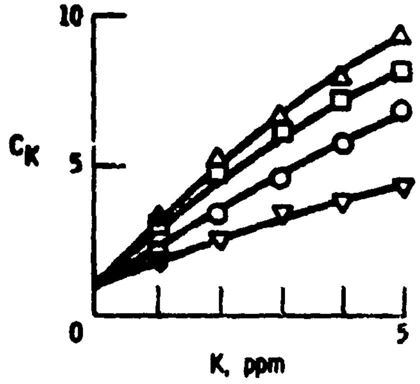

(b) POTASSIUM.

Figure 9. - Effect of concentration on C_j.

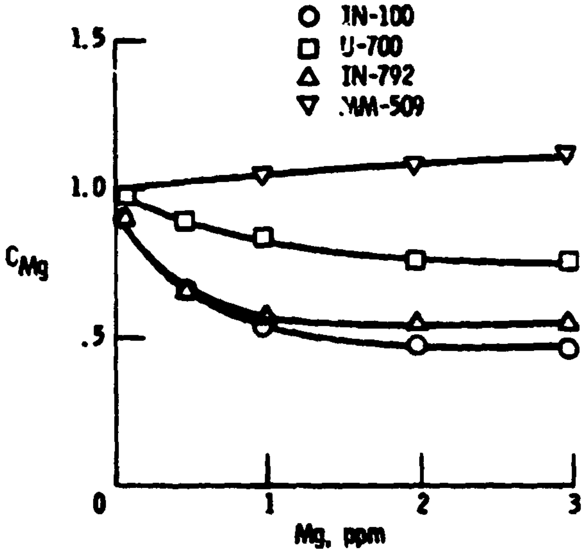

(c) MAGNESIUM.

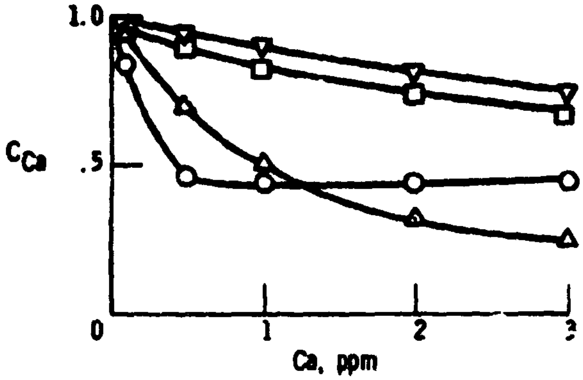

(d) CALCIUM.

Figure 9. - Continued.

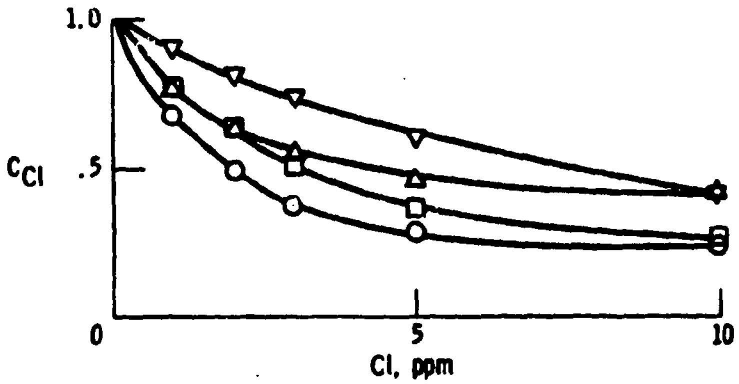

(e) CHLORINE.

Figure 9. - Concluded.

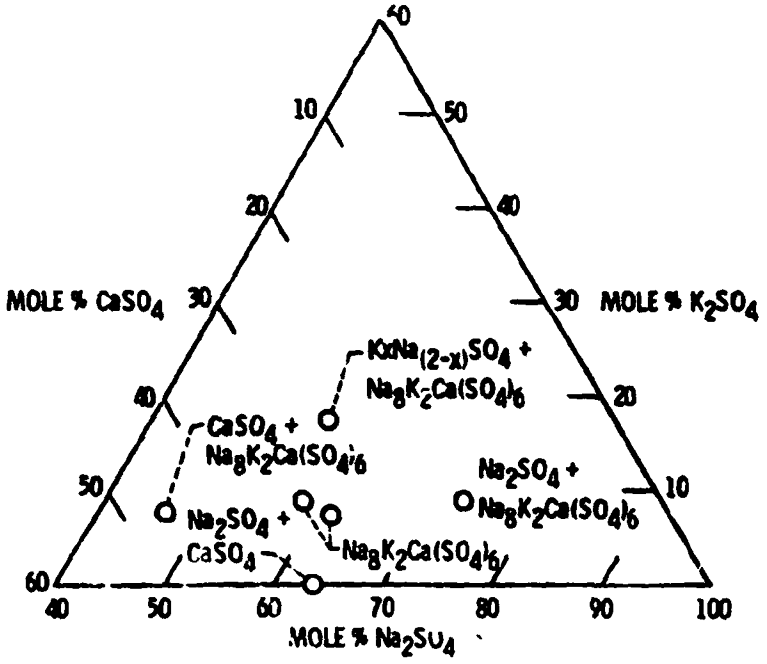

Figure 10. - Sulfate phase map.